buildings

MDPI

Review

Thermal Environment Assessment for Energy-Efficient Cooling in Air-Cooled Data Centers: Measurement, CFD, and Predictive Modeling

Haijun Tan [1], Shanran Wang [2,3], Wenli Liu [1] and Pin Li [1,*]

[1] School of Energy and Electrical Engineering, Qinghai University, Xining 810000, China; ys250858021285@mailbox.qhu.edu.cn (H.T.); 2024990040@qhu.edu.cn (W.L.)
[2] School of Aeronautic Science and Engineering, Beihang University, Beijing 100191, China; wang_shanran@buaa.edu.cn
[3] Wuhan Second Ship Design and Research Institute, Wuhan 430205, China
* Correspondence: lipin_sam@qhu.edu.cn

Abstract

Maintaining a stable thermal environment is essential for ensuring data center thermal safety and reliable operation. However, existing studies lack a systematic synthesis of thermal environment measurement, modeling approaches, and their contributions to energy-efficient cooling. This review systematically analyzes 77 studies published since 2010 on experimental measurement, CFD simulation, and predictive modeling of data center thermal environments. The review identifies representative measurement strategies at rack and room scales, analyzes factors affecting CFD reliability, and evaluates the applicability of predictive models based on experimental and simulation data. Most experimental studies focus on temperature and airflow, while only about 30.7% of the 39 experimental studies include power measurements, limiting quantitative evidence linking thermal optimization with energy performance. Among the 58 CFD studies, Fluent was used in 41.4% of cases, while 70.6% of the 17 predictive-model studies relied on CFD data for model training. CFD reliability remained sensitive to boundary conditions, model simplifications, and validation strategies. Predictive modeling was dominated by machine learning and deep learning, while reduced-order and surrogate models were also applied, enabling rapid temperature-field and thermal-risk assessment but remaining constrained by training data quality and operating condition coverage. These findings establish an integrated framework in which measurements provide empirical benchmarks, CFD extends spatial and operational understanding, and predictive models enable rapid assessment for thermal environment management and cooling energy optimization.

Keywords: data center; thermal environment; experimental measurement; CFD modeling; predictive models

Academic Editor: Yaolin Lin

Received: 13 August 2026
Revised: 22 September 2026
Accepted: 25 September 2026
Published: 28 September 2026

Copyright: © 2026 by the authors. Licensee MDPI, Basel, Switzerland. This article is an open access article distributed under the terms and conditions of the Creative Commons Attribution (CC BY) license.

1. Introduction

Driven by the rapid growth of cloud computing and artificial intelligence, data center power density has continued to rise, bringing substantial challenges to thermal management [1]. High power densities worsen local hotspots and airflow recirculation, which threatens the stable operation and reliability of IT equipment [2]. Experiments, CFD

simulations and predictive models serve as mainstream tools for data center thermal management. Rack- and room-scale thermal measurements capture temperature distribution and spatial variation, and they correlate these thermal behaviors with local air velocity [3–5]. Since experimental methods struggle to capture the full-scale thermal distribution of data centers, CFD simulations are widely employed to locate hotspots and facilitate room-scale thermal optimization [6–8]. Recent advances in machine learning and surrogate modeling have enabled accurate data center thermal prediction. By integrating limited high-fidelity experimental data with physical boundary configurations, such models achieve reliable prediction accuracy at a much lower computational cost [9–11]. Driven by inconsistent research objectives and methodological designs, findings across existing data center thermal studies are poorly comparable and transferable. Given such complex thermal environments, no single technique can fully resolve temperature and airflow distributions, thereby restricting analytical accuracy. Accordingly, an integrated framework combining experimental measurements, CFD simulations and predictive modeling is essential for high-resolution thermal characterization and systematic evaluation, which can further guide data center thermal optimization.

Experimental measurements form the basis for characterizing real data center thermal conditions and provide key data to develop and validate numerical simulations and predictive models. Experimental measurements in data center thermal studies mainly fulfill two key functions. First, measurements of temperature and air velocity are taken at rack inlets and outlets, in cold and hot aisles, and around hotspots to reveal airflow distribution and convective heat transfer characteristics. Song et al. [12] utilized multi-point temperature and air velocity measurements to show that a 1700 mm high convex deflector reduced hotspot temperatures by approximately 2 °C and improved airflow distribution. Zhang et al. [13] evaluated rack inlet and outlet temperatures, demonstrating that jet fans effectively improve data center thermal environments. Second, experimental data supply boundary conditions and validation datasets for CFD simulations to enhance model reliability. Gao et al. [14] combined experiments and CFD simulations to show the merits of local cold-aisle containment and highlight drawbacks of the Return Temperature Index (RTI) metric for assessing airflow distribution. Yu et al. [15] further validated the simulation model by experiments, demonstrating that floor-height optimization and cold-aisle containment enhances airflow uniformity and cuts energy consumption. Furthermore, studies indicate that measurement accuracy and spatial coverage impact CFD boundary conditions and data-driven model performance [16–18]. Poor accuracy or insufficient sampling coverage leads to errors in airflow simulation and prediction results. However, differences in data center configurations, operating conditions, and sensor layouts still limit the spatial coverage of experimental measurements. Most studies still rely on point measurements at representative locations, and the measured parameters vary among studies, make it challenging to fully characterize complex three-dimensional thermal environments [19–21]. Therefore, optimizing sensor arrangements to obtain high-quality thermal data under realistic constraints is critical for experimental thermal studies. Compared with experimental measurements, CFD simulations capture continuous temperature and airflow fields inside data centers at low cost and see extensive use in relevant research. Research shows numerical simulations offset the limited spatial coverage of experimental measurements and allow the evaluation of airflow and thermal performance across different operating conditions and optimization strategies. To address the limitations in spatial coverage associated with discrete sensor measurements, Singh et al. [22] used Fluent to obtain complete temperature and airflow fields and further evaluated data center energy efficiency. Similarly, Cho et al. [23] applied the 6SigmaDC platform to simulate thermal transients across six failure conditions, including cooling interruptions, supporting improvements to cooling system reliability. Cao et al. [24] adopted experimental

measurements as CFD boundary conditions to optimize rack air intake structures and reduce excessive vertical temperature differences among servers. Overall, CFD-based studies are commonly performed at multiple scales to capture facility-level temperature fields and optimize airflow organization. However, CFD predictions are highly sensitive to turbulence model selection, geometric simplification, and boundary condition configuration. Accordingly, improvements in simulation accuracy usually come with a sharp rise in computational cost, leaving the trade-off between simulation fidelity and computational efficiency yet to be properly resolved.

As data centers grow larger and more operationally complex, high computational cost of CFD simulations increasingly restricts use in rapid thermal evaluation and large-scale optimization and drives progress of data-driven thermal prediction methods. Recent studies have employed machine learning, deep learning, and reduced-order modeling to develop surrogate models of data center thermal environments, enabling rapid prediction of temperature distributions and energy consumption [25–28]. Deng et al. [29] integrated CFD with machine learning to assess various prediction models, clarify correlations between prediction accuracy and flow characteristics and achieve efficient temperature field estimation. Chen et al. [30] developed an A-PCNN model using six months of measured data and introduced a Softplus-based adaptive coefficient, reducing the MAE by 17.3% for 15 min predictions and 79.2% for 7-day predictions. These studies prove data-driven methods greatly boost computational efficiency and maintain accuracy comparable to CFD simulations. Model performance relies heavily on training data quality and geometric layouts, and accuracy declines notably in regions with strong turbulence. In addition, existing works adopt different standards for prediction accuracy, sample size and input parameters. This difference prevents direct performance comparison and restricts broader application of relevant methods.

Experimental measurements, numerical simulations, and data-driven models possess unique strengths in data fidelity, spatial resolution, and practical applicability. Nevertheless, most existing studies only adopt pairwise validation frameworks, such as experiment–CFD and CFD–prediction coupling. This partial integration focuses on improving accuracy for individual methods, and rarely forms a complete validation framework uniting all three approaches [31–35]. The complementary merits of field measurements, CFD simulations and data-driven models are not fully leveraged. Individual or combined approaches lack holistic data integration, hindering a good balance between physical fidelity and full-scale applicability in complex data center thermal analysis. Therefore, developing a unified framework that integrates experimental monitoring, CFD, and data-driven prediction helps standardize multi-source data and ensure physically consistent and reliable predictions.

Existing reviews have generally focused on data center cooling technologies, airflow management, and modeling approaches. Lu et al. [36], Chu et al. [37], and Jin et al. [38] reviewed airflow management strategies, CFD modeling methods, and simulation tools, with emphasis on airflow optimization and numerical simulation for thermal environment improvement. Zhao et al. [39] and Zhang et al. [40] reviewed cooling optimization from the perspectives of hotspot mitigation, cooling technologies, and intelligent control, while Ahmed et al. [41] further examined energy modeling and reliability assessment. However, many of these reviews focus primarily on individual technical aspects, with limited systematic analysis of the links among experimental measurement, CFD simulation, and predictive modeling. In particular, measurement parameters and sensor layouts for different research objectives, CFD reliability and validation requirements, and the data sources and applicability of predictive models have not been systematically examined. Therefore, this review systematically links measurement, CFD, and predictive modeling to examine their roles, data dependencies, and validation requirements in thermal

environment assessment and cooling optimization in air-cooled data centers, providing guidance for method selection and application.

Although field measurements, numerical simulations and predictive modeling have developed rapidly, the three techniques still adopt separate research objectives and parameter systems. This absence of unified standards makes it difficult to compare results across different studies. To fill this methodological gap, relevant indicators and evaluation criteria need to be systematically sorted and standardized. This paper reviews 77 publications on data center thermal environments published since 2010 and conducts a comparative analysis of experimental testing, CFD simulation and data-driven prediction. By exploring the interconnections between the three methods, this study constructs a unified framework to facilitate integrated thermal analysis and airflow optimization for data centers.

2. Methodology

2.1. Search Strategy

This review searched and screened studies published from January 2010 to May 2026 on thermal environment measurements, CFD simulations, and predictive modeling in air-cooled data centers. The literature search was performed using Scopus, Web of Science, IEEE Xplore, ScienceDirect, Google Scholar, and CNKI. The search terms included "data center airflow measurement," "data center CFD simulation," "data center thermal environment," "AI-based thermal management," and "predictive modeling data center," combined with "AND" and "OR" operators. The screening procedure is presented in Figure 1.

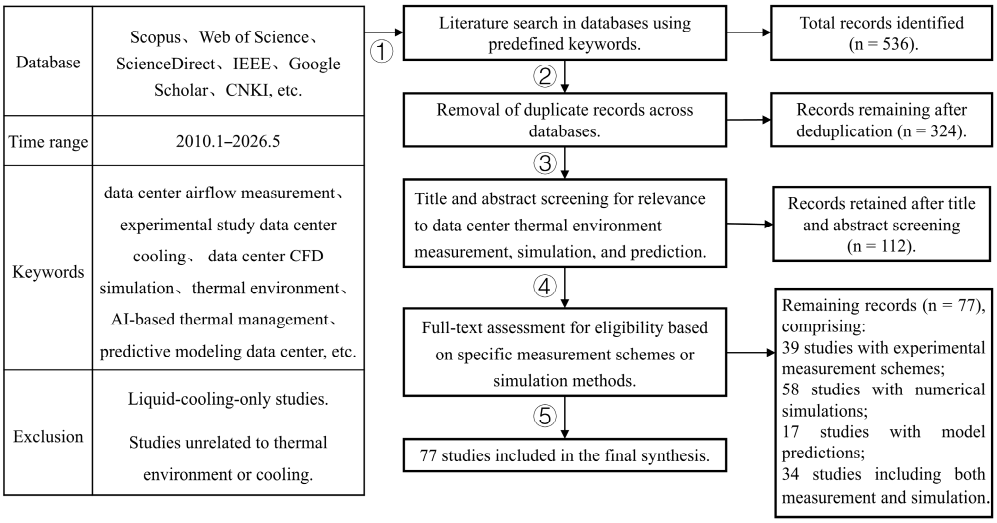


Figure 1. Flowchart of the literature screening process. Numbers ①–⑤ indicate the five stages of the process.

Data centers using air cooling as the primary heat dissipation method were included in this review. The inclusion criteria were: studies related to thermal environments in air-cooled data centers or server rooms; studies involving temperature fields, airflow organization, hotspot identification, cooling optimization, energy evaluation, or thermal environment prediction; studies using experimental measurements, CFD simulations, predictive modeling, or their combinations; and studies providing sufficient information on measurement parameters, model configurations, validation methods, training data, or evaluation metrics. Studies focusing only on liquid-cooled data centers, IT performance, network communication, or cloud computing scheduling without thermal environment

or cooling analysis were excluded. After duplicate removal, title and abstract screening, and full-text review, 77 studies were included, including 39 experimental studies, 58 CFD studies, and 17 predictive modeling studies. Since some studies involved multiple methods, these categories were not mutually exclusive.

2.2. Methodology and Objectives

The review examined three approaches used to study thermal environments in data centers: experimental measurement, CFD simulation, and predictive modeling. For each approach, key information was extracted, including measurement variables and sensor layouts; CFD boundary conditions, mesh settings, rack models, and validation variables; and training data sources, model inputs and outputs, and evaluation metrics. Their applicability and limitations were assessed through quantitative analysis, cross-study comparison, and qualitative synthesis.

This review defines the roles and limits of experimental measurement, CFD simulation, and predictive modeling in the analysis of data center thermal environments and energy performance. Experimental measurements provide actual operating parameters; validated CFD extends spatial thermal information across multiple operating conditions; and predictive models enable rapid prediction of temperature, hotspot risk, and energy performance indicators from measured or simulated data. Because improved thermal conditions do not necessarily reduce cooling energy use, energy performance should be evaluated using measured power, cooling energy data, or system-level energy models.

This review makes three main contributions. First, it proposes a tiered measurement framework for thermal safety, airflow diagnosis, and cooling energy efficiency assessment, and evaluates the strength of direct and indirect evidence provided by thermal environment indicators for energy-saving claims. Second, it establishes a CFD credibility assessment approach based on boundary condition sources, rack-model simplification, validation variables, and spatial coverage, clarifying the research questions that different simulation outputs can reliably address. Third, it develops an integrated measurement–CFD–prediction pathway showing how the three methods jointly support thermal safety assessment, hotspot detection, strategy screening, and cooling energy efficiency optimization.

3. Experimental Measurement and Analysis in Data Centers

3.1. Links Between Measurements, Thermal Metrics, and Cooling Energy Use

Experimental measurements are used to capture temperature, airflow, and energy-related parameters under actual operating conditions, supporting thermal safety assessment and airflow diagnosis [3,5]. They also provide boundary conditions and validation data for CFD models [15], and they support thermal prediction and cooling energy analysis [14–16]. Figure 2 illustrates the relationships among measured parameters, thermal environment metrics, and cooling energy use, highlighting how different measurements and indicators support cooling energy assessment.

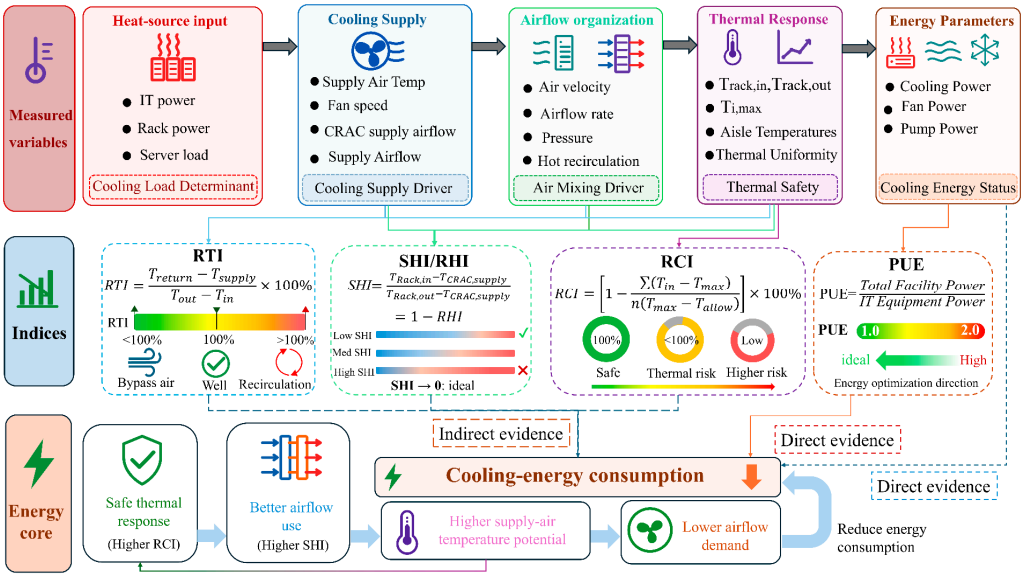


Figure 2. Relationships in data center experimental measurements [42].

Measured parameters generally cover heat input, cooling supply, airflow distribution, thermal response, and energy use. IT power determines the cooling load, while supply-air temperature and airflow rate indicate cooling capacity; airflow parameters further reveal cold-air distribution and hot-air recirculation [3,43]. Rack inlet temperature is a key indicator of thermal response and equipment safety [42], whereas cooling system power and Power Usage Effectiveness (PUE) provide direct evidence of energy performance [44]. Temperature alone can characterize thermal conditions, but without airflow data it cannot fully explain their causes or effects on cooling energy use.

The Rack Cooling Index (RCI), Return Temperature Index (RTI), Supply Heat Index (SHI), Return Heat Index (RHI), and PUE are widely used to convert temperature, airflow, and power measurements into comparable thermal and energy performance metrics. RCI is derived mainly from rack inlet temperatures and indicates compliance with recommended or allowable limits [42]. RTI, SHI, and RHI combine supply, return, rack inlet, and rack outlet temperatures to characterize supply-air matching, bypass airflow, hot-air recirculation, and return-air utilization [43,45]. PUE, the ratio of total facility power to IT equipment power, indicates system-level energy efficiency and, together with measured power or energy use, reveals the energy impact of cooling strategies [5,44]. Together, these metrics extend point measurements to broader assessments of thermal safety, airflow utilization, and system energy efficiency.

Thermal environment metrics are not direct proxies for cooling energy use. Lower inlet temperatures, higher RCI, RTI closer to its target range, lower SHI, or higher RHI generally indicate greater thermal safety margins, improved airflow management, or more effective use of supplied cooling [43]. However, such improvements may require lower supply-air temperatures, higher airflow rates, or faster fan operation, which do not necessarily reduce cooling energy use [2,5]. For example, Meng et al. [2] mitigated local hotspots by increasing ventilation and lowering the supply-air temperature, but this increased energy use. Therefore, cooling energy performance should be evaluated using measured power or energy data, PUE, or system-level energy models rather than thermal metrics alone.

3.2. Classification of Data Center Experimental Measurement Data

Table 1 summarizes 39 experimental studies by facility scale, measured variables, sensor layout, and data use. Most examined laboratory test beds or small facilities below 500 kW for model validation, boundary condition definition, thermal diagnosis, and

design optimization [2,8,22]. Medium-scale facilities between 500 kW and 5 MW and large facilities above 5 MW were seldom studied.

As shown in Figure 3, temperature was measured in all studies, followed by air velocity in 26 and power in 12. Airflow rate, humidity, and pressure were reported in 10, 6, and 3 studies, respectively. Temperature was typically measured using thermocouples, temperature–humidity sensors, or infrared thermography, whereas air velocity was measured with hot-wire or vane anemometers [19]. Power meters, airflow hoods, hygrometers, and pressure sensors were used for the remaining variables. Temperature dominates because it is inexpensive, easy to measure, and directly relevant to equipment safety. Other measurements require more instrumentation and data synchronization, limiting analysis of thermal–energy interactions [5,19].

Power measurements, however, are particularly important for linking thermal conditions with actual energy use. As discussed in Section 3.1, improvements in temperature or airflow do not necessarily indicate lower cooling energy use. Power measurements can therefore provide direct evidence of the energy effects of changes in thermal conditions and airflow. Current studies mainly focus on temperature and airflow, while power measurements remain limited. Future experiments should therefore include more measurements of power and other energy-related parameters to better quantify cooling energy performance.

Figure 4 summarizes sensor number, room area, rack count, and rack power. Figure 4a shows no clear relationship between sensor number and room area, indicating that sensor deployment depends more on study objectives, scale, and accuracy requirements than on floor area alone. As the scale expands from rack to room level, sensor number, spatial coverage, and test duration generally increase. Figure 4b further shows that most studies concern controlled test beds or rooms below 256 m^2, with rack power typically below 10 kW, although the data remain widely dispersed. Measurements in large-scale, high-power facilities with complex airflow remain limited [1].

Overall, existing measurements support thermal safety assessment and model validation [46,47] but remain dominated by temperature, with limited coverage of airflow rate, pressure difference, and power. Most studies therefore provide direct evidence of thermal performance, while direct experimental evidence of cooling energy use remains limited. Coordinated measurements of IT load, cooling-system power, and relevant operating conditions are needed to better quantify cooling energy use and the energy effects of thermal environment optimization [44].

Table 1. Statistical summary of experimental measurement data.

Reference	Facility Scale	Measuring Parameters						Layout of Measuring Points and Spatial Resolution						Uses of Experimental Data			
		T	RH	Vel	Q	Pw	Pres	No. of Points	Scale	x	y	z	Time	B	V	D	O
Song et al. (2021) [12]	Small-scale Data Center (11 m × 10.4 m × 3 m)	√		√				66	Rack		√	√	60 min		√		
Yuan et al. (2018) [48]	Small-scale Data Center (11.0 m × 8.0 m × 4.0 m)	√		√				12	Rack			√	90 min	√	√	√	
Yuan et al. (2019) [7]	Small-scale Data Center (11.0 m × 8.0 m × 4.0 m)	√		√				6	Rack			√	150 min	√	√	√	√
C.Gao et al. (2015) [14]	Small-scale Data Center (23.5 m × 13 m)	√			√	√		12	Rack	√	√		\	√			
Dogan et al. (2022) [49]	Experimental-scale Data Center (7.89 m × 5.64 m × 3.05)	√		√				10	Rack		√		\	√	√		
Kuzay et al. (2022) [20]	Experimental-scale Data Center (5.14 m × 2.2 m × 2.2 m)	√						11	Rack			√	120 min	√	√		√

Kuzay et al. (2022) [50]	Experimental-scale Data Center (Area: 14.5 m²)	√					11	Rack		√	120 min	√	√		√
Wu et al. (2024) [21]	Experimental-scale Data Center (1.65 m × 1.2 m × 0.8 m)	√		√			40	Rack	√	√	30 min	√	√		
Szeliga et al. (2026) [18]	Experimental-scale Data Center (Area: 19.56 m²; H: 3 m)	√			√		26	Rack		√	48 h	√	√		
Tradat et al. (2020) [19]	Unreported scale Data Center	√		√	√		36	Rack	√	√	5 min				√
Fang et al. (2024) [10]	Unreported scale Data Center (11.2 m × 7.6 m × 3.5 m)	√					12	Rack	√		\	√	√		
Cao et al. (2025) [24]	Unreported scale Data Center (10 m × 8.2 m × 3.2 m)	√		√			5	Rack		√	\		√	√	
Alissa et al. (2015) [46]	Experimental-scale Data Center (Area:215 m²)	√			√	√	46	Aisle	√	√	\	√	√	√	
Guo et al. (2025) [35]	Experimental-scale Data Center (8.17 m × 7.65 m × 2.84 m)	√		√		√	130	Aisle + Rack		√	√	\		√	
Nada et al. (2016) [51]	Small-scale Data Center (6.71 m × 5.49 m × 3.0 m)	√		√			40	Aisle + Rack	√	√	\		√		
Chu et al. (2019) [52]	Small-scale Data Center (6.1 m × 2.44 m × 2.59 m)	√			√		225	Aisle + Rack		√	√	60 min		√	
Lu et al. (2020) [53]	Small-scale Data Center (11.7 m × 10.4 m × 3.0 m)	√		√			198	Aisle-level		√	√	60 min	√	√	
Tradat et al. (2021) [54]	Small-scale Data Center (Area: 215.75 m², H: 4.37 m)	√			√		55	Aisle + Rack	√	√		10 min	√	√	√	
Tang et al. (2022) [55]	Small-scale Data Center (22.8 m × 17.4 m × 6.9 m)	√	√	√	√	√	188	Aisle + Rack		√	√	30 S	√	√	√	√
Saiyad et al. (2022) [56]	Small-scale Data Center	√		√			28	Aisle + Rack		√	√	\		√	√	
Singh et al. (2025) [22]	Small-scale Data Center (24 m × 10 m × 4 m)	√	√	√		√	144	Aisle + Rack	√	√	√	4 day	√	√	√	√
Liu et al.(2023) [57]	Medium-scale Data Center	√				√	32	Aisle + Rack	√	√		15 min	√	√	√	
Deng et al. (2026) [29]	Medium-scale Data Center (22.8 m × 13.2 m)	√		√		√	121	Aisle + Rack	√	√	√	\	√	√		
Fulpagare et al. (2018) [58]	Experimental-scale Data Center (8.69 m × 6.4 m)	√		√			64	Aisle + Rack		√	√	12 h	√	√	√	
Zhang et al. (2021) [13]	Small-scale Data Center (10.9 m × 10.4 m × 3.0 m)	√		√			528	Room	√	√	√	90 min	√	√		
Khalaj et al. (2014) [59]	Small-scale Data Center (18 m × 15.9 m × 2.7 m)	√			√	√	\	Room	√	√	√	\	√	√	√	
Pardey et al. (2015) [60]	Small-scale Data Center (30.5 m × 22.6 m × 3.35 m)	√		√	√	√	652	Room	√	√	√	1 min	√	√		
Wibron et al. (2018) [47]	Small-scale Data Center (5.084 m × 6.484 m × 3.150 m)	√		√		√	38	Room	√	√	√	1 min	√	√		
Wang et al. (2019) [32]	Small-scale Data Center (95.4 m² × 2.7 m)	√	√	√			225	Room	√	√	√	60 min	√	√		√
Meng et al. (2020) [2]	Small-scale Data Center (14.5 m × 7.5 m)	√		√			126	Room	√	√	√	\	√	√	√	

Han et al. (2021) [33]	Small-scale Data Center (30.5 m × 22.6 m × 3.4 m)	√			√	√		796	Room	√	√	√	1 min	√	√		
Pico et al. (2022) [61]	Small-scale Data Center (70.92 m² × 2.8 m)	√	√	√				330	Room	√	√	√	\	√	√		
Abdelmaksoud et al. (2010) [62]	Experimental-scale Data Center (Area: 83.61 m²)	√			√			756	Room	√	√	√	\	√	√		
Le et al. (2019) [63]	Experimental-scale Data Center	√	√	√		√	√	170	Room	√	√	√	60 min	√	√		√
Fulpagare et al. (2019) [64]	Experimental-scale Data Center (8.69 m × 6.4 m)	√		√				126	Room	√	√	√	60 min	√	√	√	
Wu et al. (2024) [65]	Experimental-scale Data Center(1.65 m × 1.2 m × 0.8 m)	√		√				56	Room	√	√	√	30 min			√	√
Sarikaya et al.(2025) [66]	Experimental-scale Data Center	√		√		√		58	Room	√	√	√	1 day	√	√	√	
Cho et al. (2021) [8]	Unreported scale Data Center (Area: 162 m², H: 4.8 m)	√	√					96	Room	√	√	√	30 day	√	√	√	√
Yu et al. (2025) [15]	Unreported scale Data Center (14.75 m × 13.75 m × 3.45 m)	√		√				198	Room	√	√	√	\	√	√	√	

Notes: T: temperature; RH: relative humidity; Vel: air velocity; Q: airflow rate; Pw: power; Pres: pressure; B: boundary input; V: model validation; D: thermal diagnosis; O: optimization verification. √: reported in the study; \: not reported.

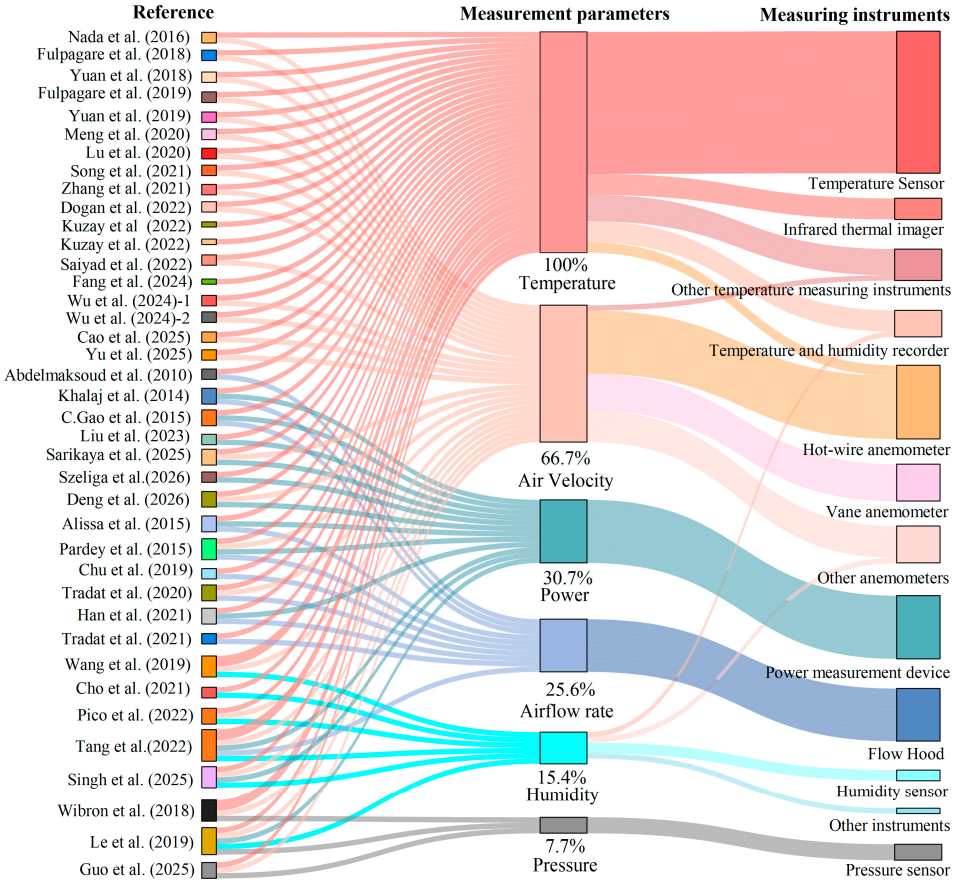


Figure 3. Measurement parameters and instruments [2,7,8,10,12–15,18–22,24,29,32,33,35,46–66].

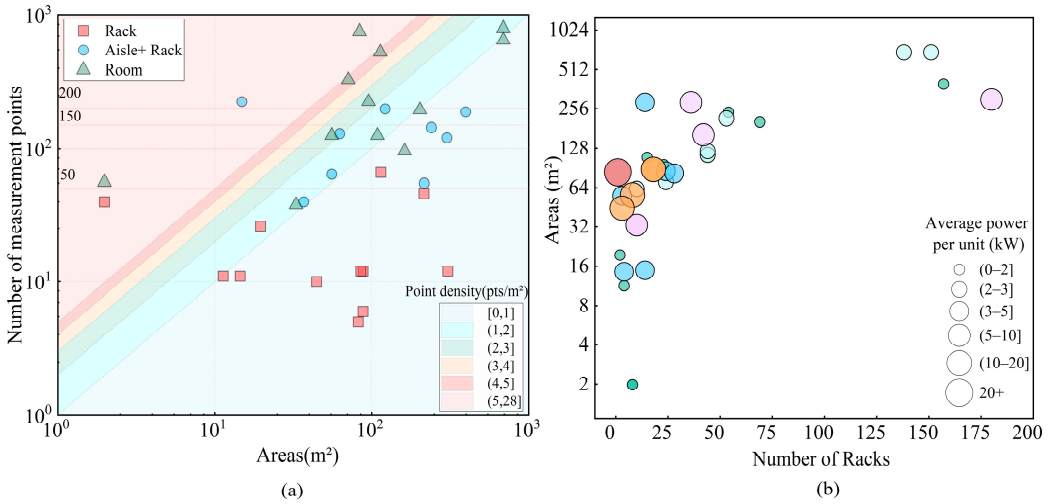


Figure 4. Experimental measurement scale and coverage: (**a**) measurement points and density; (**b**) area, rack count, and unit power.

3.3. Limitations of Existing Measurement Data

Figure 5 summarizes three common sensor layouts used in thermal environment studies. Song et al. [12] placed sensors near rack inlets and outlets to measure local temperatures and airflow, but this layout provides limited information on aisle conditions and room-wide thermal distribution. Guo et al. [35] extended the measurements to key aisle locations, enabling analysis of supply-air distribution and local airflow, although full-room circulation remained poorly captured. Zhang et al. [13] used dense temperature and air-velocity measurements at room scale to characterize the overall thermal and airflow fields, mainly for computational fluid dynamics validation and room-level assessment.

Overall, sensor layouts are largely determined by individual research objectives, with no consistent standards for variable selection or spatial deployment across scales. This limits cross-study comparison and data reuse, highlighting the need for standardized measurement frameworks tailored to different scales and assessment goals.

Table 2 summarizes experimental studies on thermal environment optimization by optimization measures, reported outcomes, and the level of support for energy assessment. To distinguish thermal performance indicators from direct energy-related evidence, the level of energy evaluation support was classified as low, moderate, or high according to the types of optimization outcomes reported in each study. Overall, existing studies mainly focus on airflow management, local flow guidance and sealing, operating-parameter adjustment, and workload distribution. Typical interventions include cold-aisle baffles, perforated-floor opening adjustments, and CRAC fan-speed control [12,54]. Reported outcomes mainly concern lower temperatures, fewer hotspots, improved temperature uniformity, and changes in RTI, SHI, RHI, or RCI. These results demonstrate improved thermal safety and airflow management but provide limited evidence on cooling energy use. Stronger energy assessment requires additional data such as supply–return temperature difference, supply airflow rate, PUE, or measured energy use [5,44].

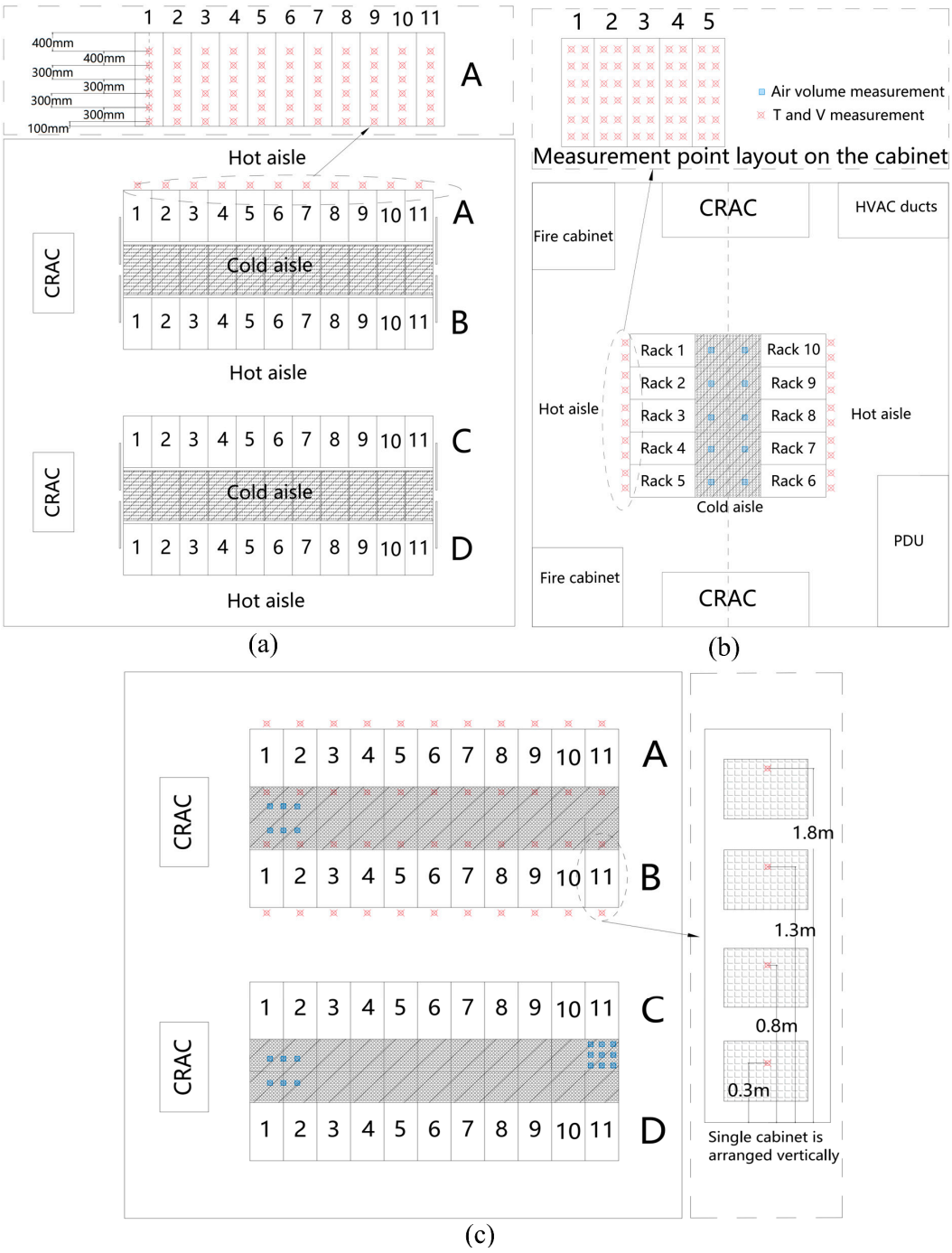


Figure 5. Schematic diagrams of several typical measurement point distributions. (**a**) It mainly focuses on the measurement of the cabinet [12]. (**b**) It mainly focuses on the measurement of the cabinet and perforated floor [35]. (**c**) It primarily focuses on measuring the cabinet, perforated floor, and hot/cold aisles [13]. Numbers 1–11 denote the rack numbers within each row, A–D denote the rack rows, and shaded areas indicate air supply through the perforated floor.

Table 2. Experimental studies on thermal optimization measures and energy evaluation.

Reference	Optimization Measures	Optimized Results				Energy Evaluation Support
		T	H	I	E	
Yuan et al. (2018) [48]	Local Flow Guidance	√	√			Low
Song et al. (2021) [12]	Local Flow Guidance	√	√			Low
Wu et al. (2024) [21]	Local Flow Guidance	√	√	√		Moderate
Cao et al. (2025) [24]	Operating Parameters	√				Low

Tang et al. (2022) [55]	Local Flow Guidance+ Operating Parameters	√	√	√		Moderate
Guo et al. (2025) [35]	Local Flow Guidance+ Load Distribution	√				Low
Singh et al. (2025) [22]	Airflow Distribution	√		√		Moderate
Zhang et al. (2021) [13]	Airflow Distribution	√	√			Low
Pico et al. (2022) [61]	Load Distribution	√			√	High
Meng et al. (2020) [2]	Local Flow Guidance			√		Moderate
Han et al. (2021) [33]	Airflow Distribution+ Operating Parameters				√	High
Cho et al. (2021) [8]	Airflow Distribution+ Operating Parameters	√			√	High
Wu et al. (2024) [65]	Airflow Distribution	√		√		Moderate
Sarikaya et al. (2025) [66]	Airflow Distribution	√	√	√		Moderate
Yu et al. (2025) [15]	Airflow Distribution	√		√		Moderate

Notes: T: temperature response; H: hotspot/temperature uniformity; I: thermal index; E: energy result. Energy evaluation support was classified as low when only T/H outcomes were reported, moderate when thermal indices (Is) were reported without quantified energy results, and high when quantified energy-related results (E) were reported. √: the corresponding result was reported.

Overall, the main limitation of existing experiments is not sensor quantity but the lack of consistent standards for measured variables, spatial layouts, and test scales [19,64]. Most studies focus on temperature, hotspots, and airflow, with limited simultaneous measurement of power, pressure difference, PUE, and system energy use [19,44,54]. The quantitative link between thermal optimization and cooling energy therefore remains unclear. Future research should move beyond isolated thermal assessment toward integrated analysis of thermal conditions, airflow, and energy performance, linking airflow interventions and thermal safety improvements to actual energy savings.

3.4. Objective-Specific Measurement Parameters and Sensor Layouts

To address inconsistent sensor layouts, limited data comparability, and weak support for cooling energy assessment, experimental measurements are organized into three levels according to data center thermal assessment needs: thermal safety assessment, airflow diagnosis and CFD validation, and cooling energy assessment. Rather than simply increasing sensor numbers, measurement zoning and parameter selection should follow objective-specific principles so that the resulting data directly support thermal characterization, airflow analysis, or energy assessment.

Figure 6 presents a representative measurement framework for thermal experiments in typical air-cooled data centers with rack-based IT equipment, raised-floor air supply, and cold/hot aisle configurations. The framework serves as a reference scheme rather than a universal measurement standard, and sensor deployment should be adjusted according to facility scale, rack arrangement, cooling configuration, and research objectives. Sensors should be placed along key airflow paths and at major heat-transfer locations, including rack inlet and outlet planes, longitudinal measurement bands in cold and hot aisles, and CRAC supply and return zones. Rack-level measurements capture intake and exhaust temperature distributions, while aisle measurements reveal temperature variations along the aisles. Measurements near the CRAC characterize supply and return conditions and link rack thermal responses to cooling-system operating boundary conditions [57,64]. Four vertical measurement levels are recommended to capture temperature stratification, while measurements at perforated floor tiles provide air velocity and airflow rate.

Together, these locations describe the overall sensor distribution and its relationship with airflow organization [54].

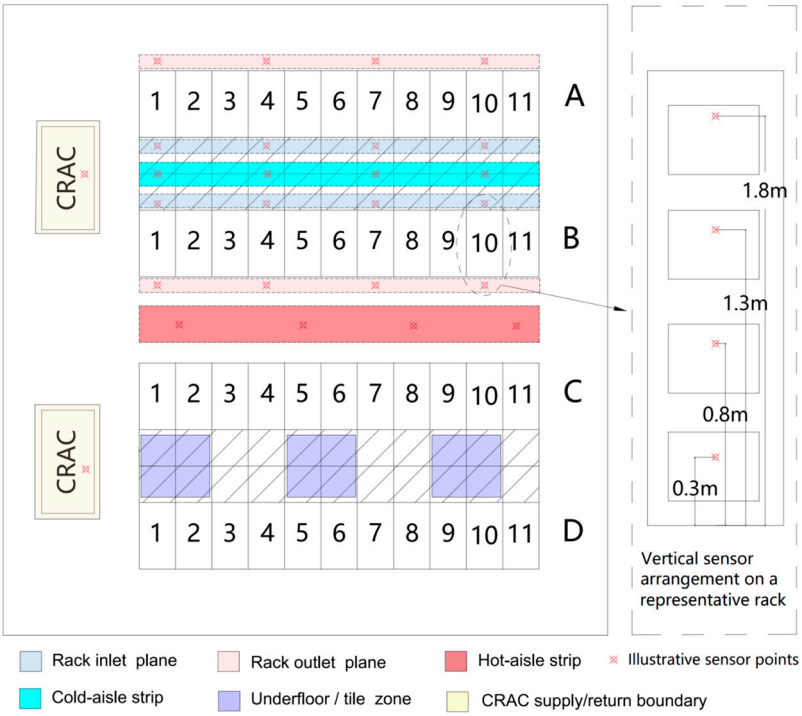


Figure 6. Recommended sensor layout for data center measurements. Numbers 1–11 denote rack numbers, and A–D denote rack rows.

In addition to thermal and airflow measurements, energy-related measurements should also be incorporated to assess the relationship between thermal performance and cooling energy use. Electrical power can be measured using power meters installed at the power supply points of IT equipment and cooling equipment. The measurements should be recorded synchronously with thermal and airflow data under the same operating conditions. The resulting power data can then be integrated over the measurement period to obtain energy consumption and relate changes in thermal performance to cooling energy use. This provides a more direct basis for assessing the energy implications of thermal performance improvements.

Table 3 summarizes representative measurement zones, core variables, supported analyses, and data requirements for the three assessment levels. Thermal safety assessment relies mainly on temperature and relative humidity to identify hotspots and determine whether rack inlet temperatures remain within recommended or allowable limits [42]. Airflow diagnosis and CFD validation additionally require air velocity, airflow rate, and pressure difference to identify bypass airflow, hot-air recirculation, and cold–hot air mixing [54]. Cooling energy assessment requires synchronized measurements of IT load, rack power, supply–return air temperature difference, CRAC operating conditions, and, where available, cooling power or energy use. These data are necessary to avoid inferring energy savings from temperature improvement alone [5,55].

Overall, measurement design should move beyond isolated temperature-field characterization toward an integrated framework that jointly supports thermal assessment, airflow diagnosis, and cooling energy evaluation. Such a framework provides a common data basis linking on-site operation, CFD validation, and predictive model training, thereby coordinating measurement, simulation, and prediction.

Table 3. Goal-oriented measurement configuration for data centers.

Objective	Representative Zones	Core Parameters	Supported Analysis	Data Requirement
Thermal safety	Rack inlet/outlet; cold/hot aisles; CRAC boundary	T, RH	Hotspots; RCI; temperature range	Typical or high-risk operating conditions
Airflow/CFD	Tiles; plenum; return path	T, v, Q, Δp	recirculation; RTI; SHI/RHI; CFD validation	Steady operation and consistent boundaries
Energy	Thermal/airflow zones; IT/rack power;	T, ΔT, Q proxy, IT power	Cooling load; energy performance; savings verification	Time-synchronized load, thermal, airflow, and energy data

Notes: T = temperature; RH = relative humidity; v = air velocity; Q = airflow rate; Δp = pressure difference; ΔT = supply–return temperature difference. Representative zones refer to measurement planes, strips, or sensor groups.

4. CFD Modeling of Thermal Flow Field Within Data Centers

4.1. Classification and Organization of CFD Modeling in Data Centers

Table 4 summarizes 58 CFD studies of data center thermal environments, covering facility scale, mesh density, boundary conditions, rack representation, and model validation. Most studies focus on small facilities or laboratory test beds, with mesh densities ranging from approximately 112 to 41,361 cells/m^3. Boundary conditions commonly include temperature, air velocity, airflow rate, and equipment power. Reported temperatures range from 5 to 35 °C, air velocities mainly from 0 to 15 m/s, and airflow rates from 0 to 41.67 m^3/s. These wide ranges reflect substantial differences in facility scale, operating conditions, and modeling assumptions [57].

Racks are commonly represented using porous-medium or black-box models to reduce computational cost. Although these simplifications reduce modeling complexity, they cannot fully represent internal rack airflow, server heat dissipation, and local flow resistance [35,65]. Model validation remains largely focused on temperature fields. Among the reviewed studies, 35 used experimental measurements, while 16 conducted benchmark comparisons against published literature. Regarding validation scale, 27 were assessed using three-dimensional spatial data, whereas the remainder relied on pointwise or two-dimensional field validation. Error metrics also vary across studies: Across the reviewed studies, reported relative errors ranged from 0.22% to above 30%, with most values remaining below 20%, absolute temperature errors from 0.1 to 4 °C, and only a few studies evaluate airflow predictions using velocity errors [47].

Figure 7 summarizes the software platforms and turbulence models used in the 58 CFD studies included in this review. Fluent was the dominant platform, appearing in 24 studies and accounting for 41.4% of the CFD studies, followed by 6SigmaDC in 12 studies. OpenFOAM, STAR-CCM+, Airpak 3.0, ANSYS CFX, and FloTHERM were used less frequently. Fluent is favored for its mature solver architecture and flexible UDF capabilities, which provide a good balance between numerical stability and engineering modeling efficiency. OpenFOAM offers greater openness and extensibility but requires more complex model development and remains less widely applied in data center research. By contrast, 6SigmaDC is tailored to data center thermal management and has considerable value for engineering design and optimization.

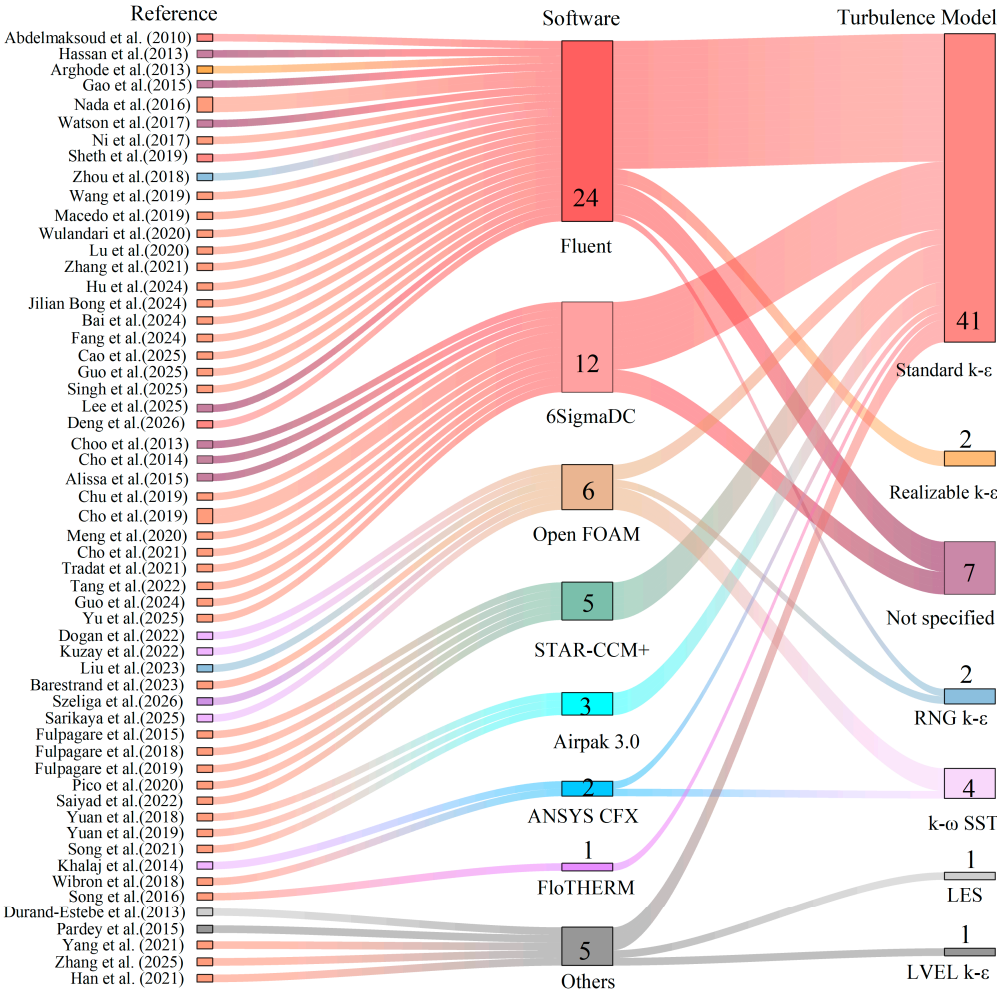


Figure 7. CFD software and turbulence model use. Numbers indicate the number of reviewed studies using each software or turbulence model. [2,7,8,10,12–14,17,18,22–24,29,31–33,35,43–64,66-84].

Among the 58 CFD studies, the standard k–ε model was used in 41 studies, accounting for approximately 70.7% of CFD studies, whereas the RNG k–ε, realizable k–ε, SST k–ω, and LES models were less common. This dominance stems from stable convergence, low computational cost, and extensive engineering validation, making the standard k–ε model suitable for most room-scale thermal predictions [47]. However, its isotropic turbulence assumption has certain limitations in representing anisotropic flow structures, including server exhaust jets, cold–hot air mixing, and local recirculation. For high-heat-density racks or detailed local flow analysis, higher-fidelity models such as SST k–ω and LES may be adopted to further improve predictive capability.

Figure 8a shows that computational domain volumes generally range from several tens to about 1000 m^3, with mesh counts typically between 10^5 and 10^7. The large variation at similar domain volumes indicates that mesh resolution is governed more by the research objective and required local detail than by domain size alone. Coarser meshes may be sufficient for evaluating overall temperature distributions in cold and hot aisles, whereas server exhaust jets, local hotspots, and recirculation require local refinement. Mesh design therefore reflects a trade-off between computational cost and prediction accuracy rather than a simple increase in cell number [47,66].

As shown in Figure 8b, among the 58 CFD studies reviewed, porous-medium and black-box models accounted for approximately 36% and 31% of the rack modeling approaches, respectively. Black-box models offer simple implementation and high

computational efficiency, making them suitable for room-scale thermal environment analysis and large-scale parametric optimization. Porous-medium models additionally represent internal flow resistance and provide more accurate predictions of rack pressure drop, airflow distribution, and hot-air recirculation. Their use has gradually increased in recent years. Driven by advances in GPU-accelerated computing, higher-fidelity server models are expected to become increasingly practical and may gradually replace conventional simplified models.

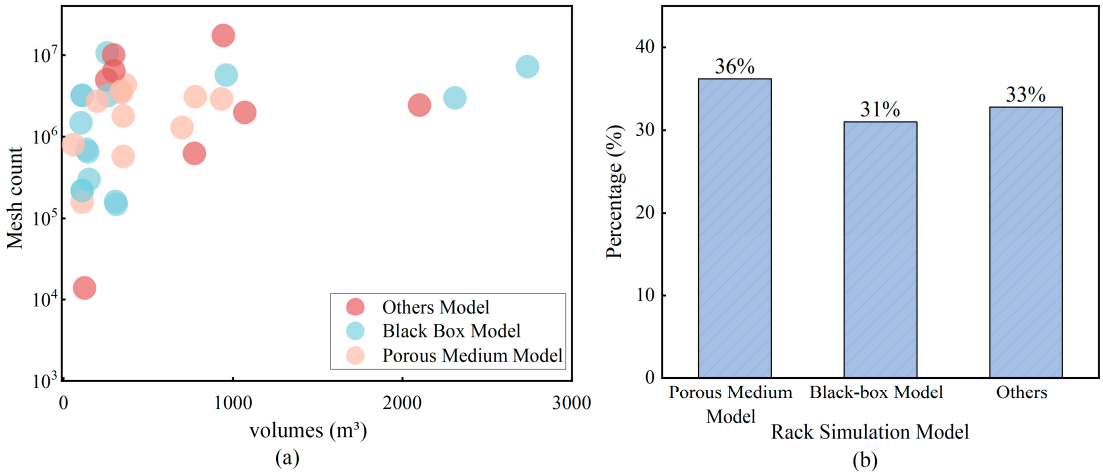


Figure 8. Statistics of server modeling methods and computational scale in data center CFD studies: (**a**) relationship between computational domain volume and mesh count; (**b**) usage proportion of different server modeling approaches.

Overall, data center CFD modeling has established a relatively mature engineering foundation, with method selection reflecting trade-offs among computational cost, physical accuracy, and practical applicability. Software platforms and turbulence models define the basic solution framework, mesh size and modeling scale determine spatial resolution, and simplifications of racks and cooling terminals affect the representation of local thermal conditions and airflow paths. The quality of CFD data should therefore be further assessed in relation to boundary condition sources and the rigor and spatial coverage of model validation.

Table 4. Statistical summary of the reviewed CFD simulations.

Reference	Facility Scale	Mesh Density	Rack Simulation Model	Rack Simulation Model					CFD Validation					
				T (°C)	Vel (m/s)	Q (m³/s)	Pw (kw)	P (pa)	Exp.	Ref.	Error	Point	Plane	Volume
Hassan et al. (2013) [67]	Small-scale Data Center (8.05 × 7 × 2.9 m)	—	—	15~22	—	2.562	3.46	10~284	—	—	—	—	—	—
Khalaj et al. (2014) [59]	Small-scale Data Center (18 m × 15.9 m × 2.7 m)	811	—	16.5	4.725	0~0.73	219.7 (T)	—	√		—			√
Choo et al. (2013) [44]	Small-scale Data Center	—	Black Box	9–14	NS	NS	313 (T)	NS	√		10%			√
Gao et al. (2015) [14]	Small-scale Data Center (23.5 m × 13 m × 3.5 m)	1860	—	16.8	—	3.66–4.77	51.94 (T)	—	√		1.9%~18.6%	√		
Pardey et al. (2015) [60]	Small-scale Data Center	1298	Black Box	21.6~27.4	—	0.252	1.1	—	√		1.9 °C			√

	(30.5 m × 22.6 m × 3.35 m)													
Nada et al. (2016) [45]	Small-scale Data Center (6.71 m × 5.49 m × 3.0 m)	29,140	Black Box	12	—	NS	3.5	10~284		√	—		√	
Nada et al. (2016) [51]	Small-scale Data Center (6.71 m × 5.49 m × 3.0 m)	29,140	Black Box	12	—	NS	3.5	—		√	—		√	
Song et al. (2016) [31]	Small-scale Data Center (8.75 m × 6.4 m × 2.7 m)	1984	Black Box	20	—	4.4	2.4	—	—	—	—	—	—	—
Ni et al. (2017) [68]	Small-scale Data Center (10 m × 9.6 m × 3.2 m)	525	Black Box	13~21	—	2.0~5.64	13.6	—		√	—	—	—	—
Sheth et al. (2019) [69]	Small-scale Data Center (71 m × 5.49 m × 3 m)	1433	Porous Medium	12.3	1	0.0713	NS	0	√		12.07%	√		
Yuan et al. (2018) [48]	Small-scale Data Center (11.0 m × 8.0 m × 4.0 m)	1633	Porous Medium	22	2.67	0.96	2.52	—	√		—	√		
Wibron et al. (2018) [47]	Small-scale Data Center (5.084 m × 6.48 m × 3.15 m)	14,311	Black Box	19.7~20	0.59~0.62	—	0~5.326	—	√		0.0521 m/s		√	
Yuan et al. (2019) [7]	Small-scale Data Center (11.0 m × 8.0 m × 4.0 m)	5120	Porous Medium	22	2.67	—	16.98 (T)	—	√		4%	√		
Wang et al. (2019) [32]	Small-scale Data Center (95.4 m² × 2.7 m)	41,361	Black Box	18	0.72	4.33	0~2.95	—	√		6%			√
Chu et al. (2019) [52]	Small-scale Data Center (6.1 m × 2.44 m × 2.59 m)	—	Porous Medium	20~25	—	8.61	4	NS	√		—	√		
Meng et al. (2020) [2]	Small-scale Data Center (14.5 m × 7.5 m × 3 m)	—	—	23	0.8~1.8	4.45	37.49 (T)	—	√		0.22%~4.29%			√
Lu et al. (2020) [53]	Small-scale Data Center (11.7 m × 10.4 m × 3.0 m)	11,860	Porous Medium	16~20	—	3.5	2	—	√		—		√	
Zhang et al. (2021) [13]	Small-scale Data Center (10.9 m × 10.4 m × 3.0 m)	10,296	Porous Medium	18	2	3.5	2	NS	√		5%		√	
Tradat et al. (2021) [54]	Small-scale Data Center (215.75 m², H: 4.37 m)	18,455	—	10.4~18.8	—	7.79~8.165	120 (T)	—	√		1.6 °C		√	
Song et al. (2021) [12]	Small-scale Data Center (11 m × 10.4 m × 3 m)	10,498	Porous Medium	18~22	—	3.5~5.4	1.8~4.2	—	√		5%			√
Han et al. (2021) [33]	Small-scale Data Center	—	Black Box	15~24	—	0.14~41.67	344(T)	—	√		10%			√

	(30.5 m × 22.6 m × 3.4 m)													
Tang et al. (2022) [55]	Small-scale Data Center (22.8 m × 17.4 m × 6.9 m)	2646	Black Box	17.8	—	9	291.46 (T)	—	√		12%		√	
Pico et al. (2022) [61]	Small-scale Data Center (70.92 m² × 2.8 m)	13,768	Porous Medium	NS	NS	2.93	2~7	—	√		20%			√
Saiyad et al. (2022) [56]	Small-scale Data Center	—	Porous Medium	17	1.54	—	10	0		√	1.4 °C			√
Guo et al. (2024) [70]	Small-scale Data Center (32.8 m × 16.9 m × 5 m)	—	—	22	—	0.36~0.465	6.3	—		√	—			√
Singh et al. (2025) [22]	Small-scale Data Center (24 m × 10 m × 4 m)	5946	Black Box	18	2.8/3.7	—	NS	NS	√		1.1 °C			√
Yu et al. (2025) [15]	Small-scale Data Center (14.75 × 13.75 × 3.45 m)	1851	Porous Medium	18	—	8.5	0~6.07	0.031~14	√		9.44%			√
Cho et al. (2014) [43]	Medium-scale Data Center (10.8 m × 15 m)	—	—	13~22	—	6.94–7.78	4	—	—	—	—	—	—	—
Macedo et al. (2019) [71]	Medium-scale Data Center	—	Porous Medium	NS	0~1	—	0.34~0.892	0	—	—	—	—	—	—
Cho et al. (2020) [17]	Medium-scale Data Center (34.16 × 12.8 × 4.8 m)	1166	—	15	4~10	10.8	8.8~16	—	—	—	—	—	—	—
Liu et al. (2023) [57]	Medium-scale Data Center	—	Black Box	23~35	—	NS	0.159~0.304	—	√		0.7 °C		√	
Deng et al. (2026) [29]	Medium-scale Data Center (22.8 m × 13.2 m)	—	Porous Medium	18–27	5.5–9.5	—	55.9~134.5 (T)	NS	√		3.81%			√
Zhang et al. (2025) [72]	Medium-scale Data Center (33.6 m × 13.2 m × 4.5 m)	1563	—	20~25	—	13.89	3	—	√		1.5 °C			√
Cho et al. (2019) [23]	Large-scale Data Center (544.3 m²)	—	—	22	—	3.5	4	—	—	—	—	—	—	—
Abdelmaksoud et al.(2010) [62]	Experimental-scale Data Center (15.24 × 5.49 × 3 m)	19,594	—	12.6	1.0~5.07	4.81	23	—	√		2 °C			√
Durand-Estebe et al. (2013) [73]	Experimental-scale Data Center (2.4 × 3 × 3.0 m)	—	Porous Medium	17~30	—	0.08	3	—		√	0.27 °C		√	
Alissa et al. (2015) [46]	Experimental-scale Data Center (area 215 m²)	—	Porous Medium	—	10–15	7.79	—	NS	√		3%		√	
Fulpagare et al. (2015) [74]	Experimental-scale Data Center (8.5 ×12.2 ×3 m)	479	Black Box	15	12.74	4.91	10	0		√	33%	√		
Fulpagare et al. (2018) [58]	Experimental-scale Data Center (8.69 m × 6.4 m)	—	Porous Medium	17	1.54	3	10	0	√		—			√
Zhou et al. (2018) [75]	Experimental-scale Data Center	—	Porous Medium	5/7	—	0~0.1	0.3	0~150		√	2 °C	√		

Fulpagare et al. (2019) [64]	Experimental-scale Data Center (8.69 mx6.4 m)	—	Porous Medium	17	1.54	0.15	10	0	√		—			√
Yang et al. (2021) [76]	Experimental-scale Data Center	—	—	22	—	0.72-~2.88	17	—		√	—	√		
Dogan et al. (2022) [49]	Experimental-scale Data Center (7.89 × 5.64 × 3.05)	5158	Black Box	17	5	3.04	3.7~3.9	—		√	—			√
Kuzay et al. (2022) [50]	Experimental-scale Data Center (Area: 14.5 m^2)	—	Porous Medium	21	—	0.811	0.165~3	0	√		2.5 °C			√
Barestrand et al.(2023) [77]	Experimental-scale Data Center (6.5 × 7 × 3.15 m)	4549	Black Box	18.3	—	1.94~2.06	2.01~6.21	NS		√	0.1 °C	√		
Hu et al. (2024) [78]	Experimental-scale Data Center	—	Black Box	12	—	4~5	8~12	0		√	0.5 °C		√	
Jilian Bong et al. (2024) [79]	Experimental-scale Data Center (6.8 × 5.7 × 3.2 m)	112	—	18	—	2.36	30 (T)	—		√	—			√
Bai et al. (2024) [80]	Experimental-scale Data Center (6.71× 5.49× 3 m)	1981	Black Box	12.3	1	0.0713	3.5	0		√	0.91%			√
Guo et al. (2025) [35]	Experimental-scale Data Center (8.17 × 7.65 × 2.8 m)	—	—	20.5	NS	NS	2.0~4.5	NS	√		9.6%			√
Sarikaya et al. (2025) [66]	Experimental-scale Data Center	—	Porous Medium	23~35	—	0.02~0.13	0.128~0.982	NS	√		1.6 °C			√
Szeliga et al. (2026) [18]	Experimental-scale Data Center (Area: 19.56 m^2; H: 3 m)	13,633	Porous Medium	NS	—	0.53	NS	—	√		0.63 °C			√
Arghode et al. (2013) [81]	Unreported scale Data Center	—	—	NS	1~4	0.94	—	0		√	30.8%	—	—	—
Watson et al. (2017) [82]	Unreported scale Data Center	—	—	25	0.25	—	15	15	—	—	—	—	—	—
Wulandari et al. (2020) [83]	Unreported scale Data Center(13.68 × 7.2 × 3 m)	34,120	—	16~17	2.3	—	NS	—	√		—			√
Cho et al. (2021) [8]	Unreported scale Data Center (162 m^2, H:4.8 m)	3978	Porous Medium	15~17	—	6.94	4	—	√		3~4 °C			√
Fang et al. (2024) [10]	Unreported scale Data Center (11.2 × 7.6 × 3.5 m)	21,482	—	18~26	—	3~9	0.36~0.66	—	√		—	√		
Cao et al. (2025) [24]	Unreported scale Data Center (10 × 8.2 × 3.2 m)	12,200	Black Box	14~18	1.5~3	9.3~18.5	NS	—	√		—	√		
Lee et al. (2025) [84]	Unreported scale Data Center	—	—	10~15	0.5~0.6	—	NS	NS		√	4%			√

Notes: T = temperature; Vel = air velocity; Q = airflow rate; Pw = power; P (pa) = pressure; Exp. = experimental or in-situ measurement; Ref. = reference or benchmark data; NS = not specified. √: the corresponding result was reported.

4.2. Boundary Conditions and Model Validation

Boundary conditions and model validation are key determinants of CFD reliability in data center studies. Software platforms, turbulence models, and mesh resolution define the numerical framework, whereas temperature, airflow, heat-source, and related

boundary conditions directly affect the simulated cooling process and thermal distribution [54]. Figure 9 summarizes the boundary condition settings, validation sources, validated variables, and spatial coverage reported in previous studies.

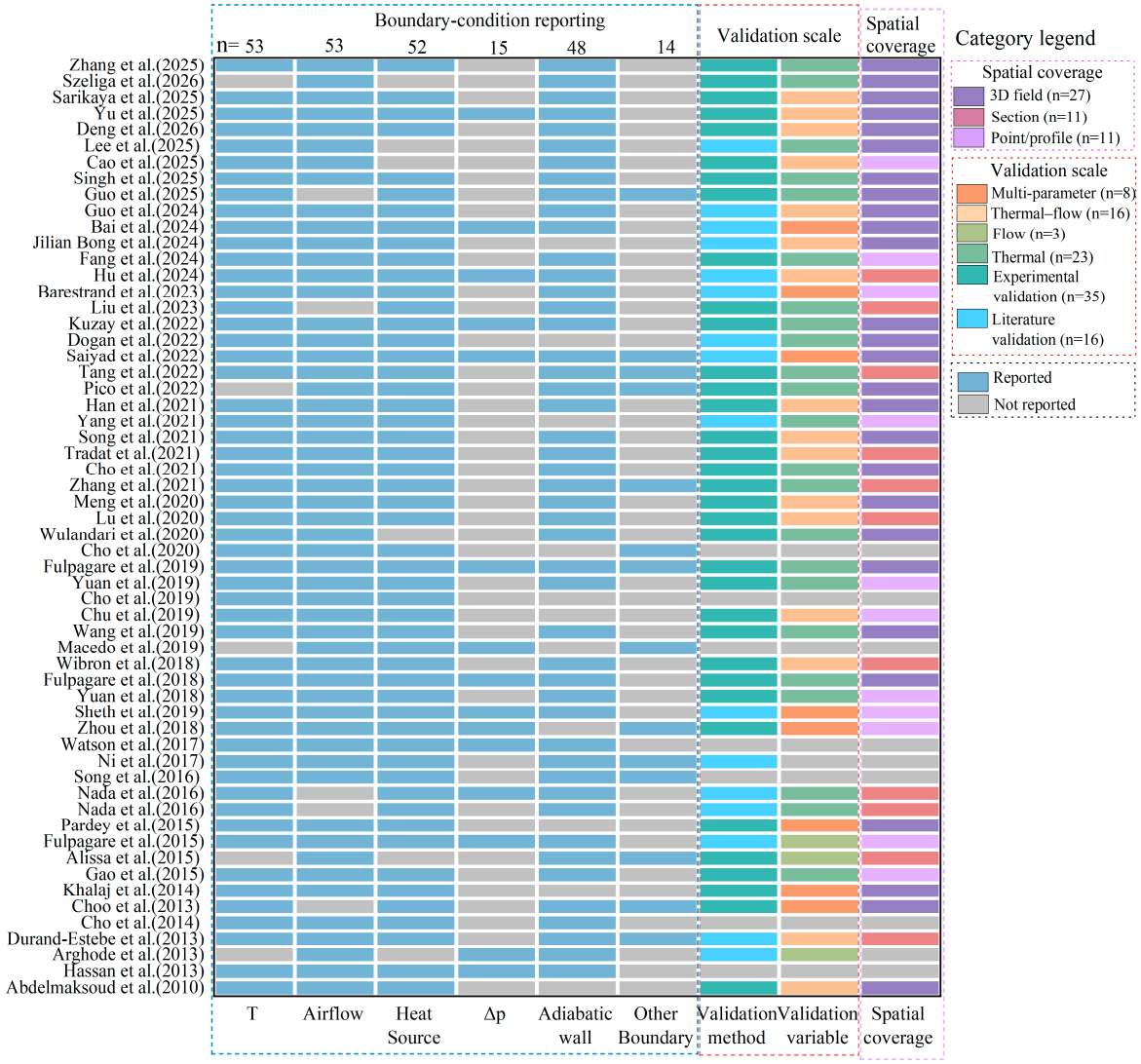


Figure 9. Boundary condition reporting and validation coverage in CFD studies [2,7,8,10,12–14,17,18,22–24,29,31–33,35,43–64,66–84].

Temperature and airflow conditions and heat-source inputs were the most common, reported in 53, 53, and 52 studies, respectively. Pressure conditions and parameters such as porosity were less frequently specified, with pressure boundaries reported in only 15 studies. In engineering studies, this likely reflects the difficulty of pressure measurement, limited access to field data, and the widespread use of default pressure-outlet settings in commercial software. However, pressure and flow resistance directly influence supply-air distribution, rack ventilation, and recirculation paths. Temperature, airflow rate, and heat-source conditions alone may therefore be insufficient to represent actual airflow processes [47].

Experimental validation was the dominant approach, used in 35 studies, followed by validation against published data in 16. Temperature fields were validated in 23 studies, while 16 jointly assessed temperature and airflow. Eight studies included other combinations of physical variables, and only three focused solely on airflow. Many studies therefore appear to regard accurate temperature prediction as sufficient evidence of CFD model reliability. This assumption has clear limitations in airflow-oriented studies because

different flow fields may produce similar temperature distributions; temperature-only validation cannot establish the fidelity of the predicted velocity and pressure fields. A hierarchical validation strategy should therefore be adopted according to the research objective: temperature validation may be sufficient for thermal safety assessment, whereas airflow analysis should also include velocity or pressure validation.

Regarding spatial scale, 27 studies used three-dimensional validation, while two-dimensional and point- or line-based validation were each reported in 11 studies. Compared with local measurements, validation over a larger spatial scale provides a more complete assessment of temperature and airflow distributions. CFD credibility thus depends not only on whether validation is performed but also on whether the selected physical variables and spatial coverage match the research objective. Overall, existing studies provide a relatively sound basis for boundary condition specification and model validation, but pressure, flow-resistance, and related boundary conditions, validation across multiple physical quantities, and spatial-scale matching still require further improvement [54].

4.3. Factors Affecting the Credibility of CFD Results

Data center CFD studies have established a relatively mature engineering basis; however, simulation credibility cannot be assessed solely from the software platform, turbulence model, or mesh count. In thermal environment simulations, mesh resolution, rack representation, and experimental validation jointly affect predicted temperature and velocity fields, as well as hotspot identification [32,47]. Figure 10 provides representative examples of how these factors affect CFD reliability.

Figure 10a presents the cold- and hot-aisle temperatures reported by Deng et al. [29] under different mesh counts. The results indicate that coarse meshes lead to larger temperature deviations, whereas predictions gradually stabilize with increasing mesh resolution. Therefore, mesh independence should be evaluated based on key thermal outputs rather than residual convergence or cell number alone. Local refinement remains particularly important around supply-air jets, hot-air recirculation regions, and high-heat-flux areas, where insufficient resolution may reduce prediction reliability [47].

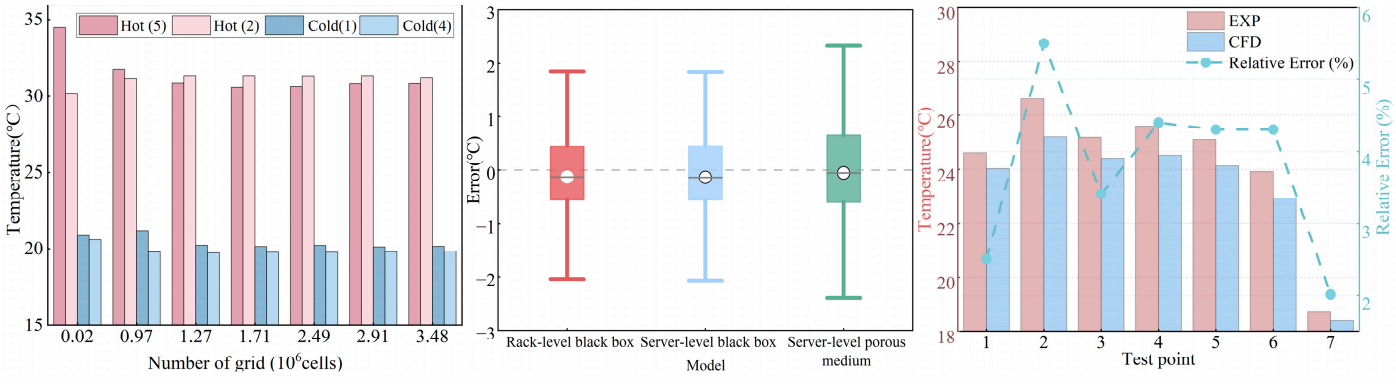


Figure 10. CFD verification and validation: (**a**) grid independence [29]; (**b**) rack model comparison [85]; (**c**) experimental validation [86].

Rack representation is another important factor affecting CFD accuracy. Figure 10b compares temperature prediction errors obtained using different rack models reported by Gong et al. [85]. The results show that different rack representations result in different levels of prediction accuracy, indicating that simplifications of internal flow resistance and heat-source distribution can influence local thermal predictions. Simplified rack models reduce computational cost for room-scale simulations but require experimental validation to confirm their applicability.

Figure 10c presents the comparison between CFD predictions and experimental measurements reported by Chen et al. [86]. The CFD model reproduces the overall temperature variation with relatively low errors, although local discrepancies remain. These deviations may arise from complex airflow structures, local recirculation, and model simplifications. CFD validation should therefore consider both prediction accuracy and spatial distribution characteristics to ensure reliable representation of the actual thermal environment.

Overall, mesh resolution, rack representation, and experimental validation are important factors affecting CFD reliability in data center thermal analysis. Their selection should be guided by research objectives and accuracy requirements, with appropriate trade-offs between computational cost and model fidelity. Reliable CFD applications therefore require suitable modeling strategies and validation approaches to support thermal environment assessment and airflow analysis [47,66].

4.4. CFD-Supported Thermal Diagnosis and Applications

Compared with field measurements, CFD provides continuous temperature, velocity, and pressure fields for thermal environment analysis, airflow diagnosis, and cooling-strategy optimization in data centers [32]. Table 5 links these outputs to their physical meaning, typical applications, and reliability requirements. For multi-condition optimization, reliability depends on both validation of the baseline model and the representativeness of the selected operating conditions.

Table 5. Physical implications, applications, and evidence requirements of CFD outputs.

CFD Output	Physical Meaning	Applications	Evidence Requirements
Temperature field	Thermal distribution and non-uniformity	Thermal safety; hotspot detection	Heat-source boundary and temperature validation
Velocity field/streamlines	Flow distribution and pathways	Airflow organization; bypass/recirculation	Airflow boundary and velocity validation
Pressure field	Pressure distribution and resistance	Air distribution and resistance analysis	Pressure/resistance data and pressure validation
Multi-condition results	Thermal response to operating changes	Parameter and strategy optimization	Validated model and representative cases

CFD directly supports thermal safety assessment and airflow organization analysis. Temperature fields identify rack inlet temperatures, cold- and hot-aisle temperatures, local hotspots, and temperature exceedance zones [12]. Velocity and pressure fields reveal supply-air distribution, hot-air recirculation, mixing between cold and hot air, and other airflow organization characteristics [43]. Temperature-validated models can generally support thermal risk assessment, whereas airflow organization analysis requires further validation of air velocity, airflow rate, pressure, or related variables [47].

CFD is also widely used for cooling-strategy optimization through supply-air parameter adjustment, rack-layout optimization, airflow organization improvement, and other measures. Parametric simulations examine how supply-air temperature, airflow rate, load distribution, and airflow organization strategies affect temperature distributions, hotspot formation, and airflow transport characteristics [45]. They can also compare thermal environment responses under aisle containment, airflow-guiding structures, supply- and return-air optimization, and other cooling schemes, providing a basis for data center cooling optimization [51,73].

CFD provides only indirect support for cooling energy assessment. Lower temperatures, fewer hotspots, or reduced hot-air recirculation indicate improvements in thermal safety and airflow organization but do not necessarily imply lower cooling energy use

[43]. CFD is therefore better suited to thermal environment diagnosis and strategy screening, while energy-related conclusions should be verified using experimental measurements, cooling-system models, or operational energy-use data [5,44]. Future CFD studies should strengthen the coupling between thermal environment prediction and cooling energy models to enhance the practical value of CFD in data center energy optimization.

5. Predictive Models for Data Center Thermal Environments

As high-density computing and dynamic workloads expand, conventional measurements and CFD are becoming increasingly costly and slow for multi-condition thermal environment prediction. Data-driven models are therefore gradually emerging as an important approach linking high-fidelity simulation with rapid decision-making, while complementing experimental measurements and numerical simulations. Building on the preceding analyses of these two methods, this section reviews model types, training data sources, sample sizes, accuracy, and computation time.

5.1. Thermal Environment Prediction Models

Table 6 summarizes 17 representative studies and compares their model types, training data sources, sample sizes, prediction accuracy, and computational efficiency. Existing studies have applied various predictive approaches, including data-driven models, reduced-order and surrogate models, and CFD-coupled hybrid models. Among these approaches, data-driven models, such as machine learning, artificial neural networks, and deep learning, represent the most commonly applied approaches among the reviewed studies due to their strong nonlinear mapping capability and relatively low computational cost [10,16,87]. These models are mainly applied for pointwise temperature and local thermal environment prediction, while deep learning methods further capture complex relationships among server power, supply-air parameters, and environmental variables for temperature-field prediction [10,11]. However, their performance relies strongly on training data quality and operating condition coverage, and their physical interpretability remains limited. Reduced-order and surrogate models mainly utilize CFD-generated samples to rapidly reconstruct temperature and flow fields [34]. They reduce computational costs for repeated simulations and optimization while retaining spatial information from CFD models, but their accuracy depends on the quality and representativeness of the CFD database. CFD-coupled hybrid models further combine physical simulations with data-driven methods to improve prediction capability under complex operating conditions.

Table 6. Statistical summary of predictive models for data center thermal environments.

Author	Algorithm	Training Data Source	Number of Training Samples	Input Parameters			Prediction Accuracy	Output Time	CFD Output Time
				IT_load	T_sup	Airflow			
Tarutani et al. (2015) [25]	ML	Experiment	17,280	√	√	√	Accuracy: 0.095 °C	10 s	—
Athavale et al. (2019) [16]	GPR	CFD	300	√	√	√	Accuracy: 0.6 °C	—	—
Asgari et al. (2021) [87]	Hybrid Surrogate mode	CFD	44	√	√	—	Accuracy < 1.5 °C	4 s	28,800 s
Tang et al. (2025) [28]	POD	CFD	32	√	√	√	Accuracy: 0.5 °C	12 min	200 h
Wang et al. (2025) [88]	CNN-BiLSTM-Attention mode	CFD	200	√	√	√	Accuracy < 0.3 °C	—	—

Athavale et al. (2018) [9]	ANN	CFD	300	√	√	√	Relative Error: 2.7%	10 s	300 min
Jin et al. (2023) [27]	POD	CFD	1819	√	√	√	Relative Error: 0.01%	30 s	120 min
Dai et al. (2024) [34]	POD + CFD	CFD	112	√	√	√	Relative Error: 0.59%	10 min	1340 min
Guo et al. (2025) [35]	FNM-CFD	CFD	60	√	√	√	Relative Error < 5%	2250 s	4440 s
Wang et al. (2022) [89]	MDF + DDF	Experiment	19,253	√	—	—	MAPE < 3.5%	1 s	—
Deng et al. (2026) [29]	CFD-ML	CFD	1259	√	√	√	MAPE < 1.44%	<2.16 min	2660.4 min
Lin et al. (2022) [26]	ML	CFD	1100	√	√	√	MAPE < 3.0%	<1 ms	—
Fang et al. (2024) [10]	CFD + ADB	CFD	8000	√	√	√	MAPE: 0.68%	97 ms	5 min
Kuwahara et al. (2018) [90]	DNN + CFD	Experiment	Continuous one-year data	√	√	√	MSE < 0.08 °C²	<1 s	30 min
Saiyad et al. (2021) [91]	ANN	CFD + Experiment	905	√	√	√	MSE: 0.68 °C²	10 s–30 s	—
Omrani et al. (2025) [92]	GA + SAEA	CFD	225	√	√	√	MSE: 0.00014 °C²	2 min	3 h
Chen et al. (2025) [30]	A-PCNN	Experiment	Continuous six-months data	√	√	√	MSE: 0.136 °C²	15 min	—

Notes: IT_load: IT thermal load; T_sup: supply-air temperature; Airflow: airflow characteristics. √: the corresponding parameter was used as a model input.

The effectiveness of these predictive approaches is closely related to the availability and quality of training data. From the perspective of data sources, training data are obtained mainly from measurements and calibrated CFD simulations. Among the 17 predictive modeling studies, CFD simulation data were the predominant source, with 12 studies accounting for 70.6% of the reviewed studies, whereas measured data were used in four studies and only one study combined both sources. CFD simulations can generate multi-condition samples under controlled boundary conditions and provide relatively complete spatial thermal environment information. CFD data have therefore gradually become the primary source for model training. Fang et al. [10], for example, generated 8000 operating condition samples using CFD to alleviate data scarcity. In contrast, measured data more closely reflect actual operating conditions and can be used to calibrate or validate numerical models. However, limitations in sensor layout, acquisition cost, and operating condition coverage usually prevent measured data alone from supporting large-scale spatial prediction [19].

Existing models are built mainly on IT load, supply-air temperature, airflow conditions, and other key inputs to map changes in operating states to thermal environment responses [87]. Their outputs mainly include temperature distributions, hotspot risks, and thermal environment indicators, supporting thermal safety assessment and cooling-strategy optimization. Compared with conventional CFD simulations, rapid prediction models can significantly reduce computational cost and enable near-real-time thermal environment prediction, supporting parameter optimization and online operational control [11]. However, because prediction targets, data sources, evaluation metrics, and other

aspects vary across studies, a common evaluation benchmark remains lacking, making direct comparisons difficult [16].

Overall, predictive models are not intended simply to replace CFD or experimental measurements. Instead, they enable rapid thermal environment prediction by combining the complementary strengths of different data sources. Future research should further establish mechanisms for integrating CFD and measured data and incorporate physical constraints to improve model generalization under complex operating conditions [87].

5.2. Factors Affecting Model Prediction

Figure 11 summarizes comparative results from representative studies. Figure 11a compares the performance of different algorithms under identical conditions reported by Fang et al. [10]. The results indicate that algorithm structure affects the capability of representing thermal environment responses. Data center thermal environments are jointly influenced by IT load, supply-air parameters, airflow organization, environmental disturbances, and other factors, resulting in strongly nonlinear input–output relationships [87]. Conventional machine learning and simple neural networks can predict point temperatures or thermal environment indicators, whereas reduced-order, surrogate, and deep learning models are more suitable for capturing multivariable coupling, reconstructing temperature fields, and rapidly predicting multiple operating conditions [11,34]. Algorithm selection should therefore match the prediction objective. Prediction performance depends not only on model structure but also on the quality and coverage of training data.

Figure 11b shows the effect of different training datasets on prediction error, as reported by Saiyad et al. [91]. CFD data provide relatively complete spatial field information and enable the generation of training samples under multiple operating conditions. However, models trained on CFD data may inherit uncertainties associated with boundary conditions, mesh resolution, and other model simplifications. Experimental or operational data more closely reflect actual conditions, but have limited spatial and operating condition coverage [32]. The thermal response learned by a model is therefore constrained by its training data; its applicability depends on both the data source and modeling scale.

Figure 11c illustrates the influence of training sample size on prediction performance reported by Deng et al.[29]. With increasing sample size, the MAE of different algorithms gradually decreases, while the R^2 values improve and tend to stabilize. This indicates that sufficient training samples contribute to improved prediction accuracy and model stability. However, simply increasing the number of samples does not necessarily guarantee continuous improvement, as representative coverage of operating conditions, including load levels, supply-air parameters, and airflow states, is more important than sample quantity alone [29].

Overall, data center thermal environment prediction performance is jointly influenced by algorithm selection, training data source and quality, and sample coverage. Future research should not focus only on algorithm complexity but should also emphasize the construction of representative training datasets, complementary use of CFD and measured data, and validation of model generalization across different operating conditions [10,57].

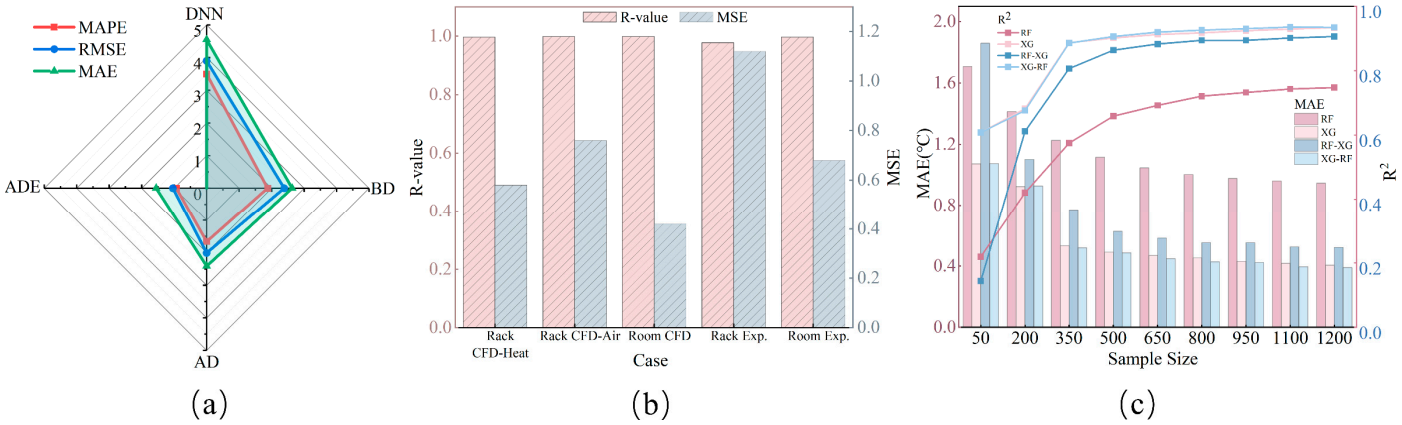


Figure 11. Factors affecting prediction performance: (**a**) model type [10]; (**b**) training data source [91]; (**c**) training sample size [29].

5.3. Analysis of Model Prediction Efficiency

In terms of computational efficiency, surrogate models outperform traditional CFD simulations by a large margin. Figure 12 compares the time consumption of CFD simulation and surrogate model prediction, with detailed time ranges listed in Table 6. CFD generally takes 5 min to 200 h for computation, while surrogate models complete predictions within 0.097 to 2250 s. CFD relies on iterative solving of complex equations and thus consumes massive computing resources. Trained surrogate models, by contrast, enable instant inference. Additionally, some studies combine reduced-order models such as POD with deep learning [34]. These methods retain key flow and heat transfer characteristics while avoiding iterative computation, further cutting computational costs. The transition from time-consuming simulation to instant prediction supports efficient evaluation of complex thermal environments, proving great application potential of surrogate models in real-time control and rapid optimization.

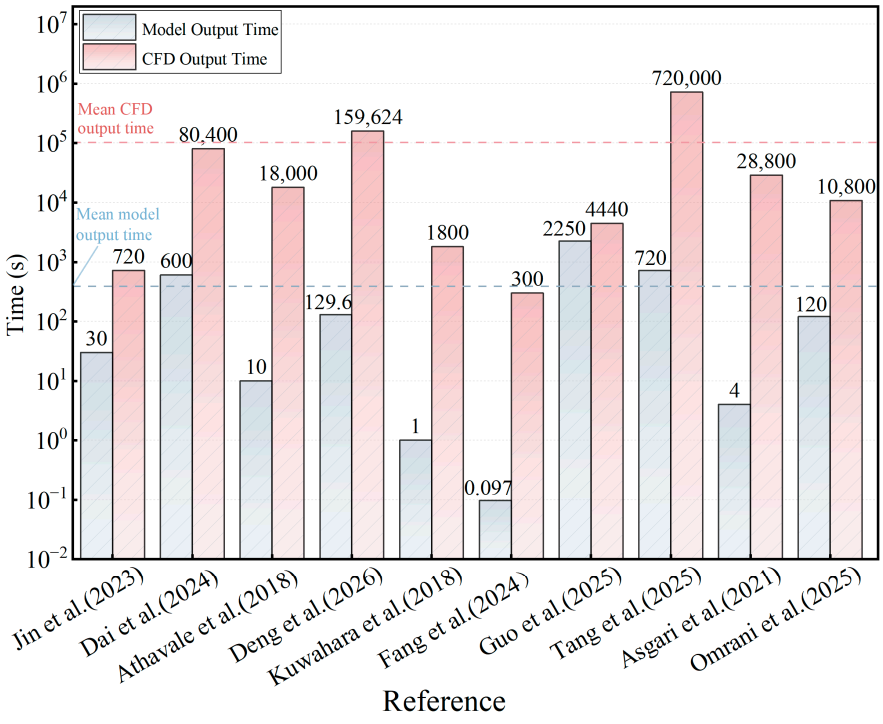


Figure 12. Comparison of output time between CFD simulations and model predictions [9,10,27–29,34,35,87,90,92]. The dashed lines indicate the mean output times of CFD simulations and model predictions.

6. Discussion

6.1. Comparison and Assessment of Experimental Measurements, CFD, and Predictive Models

Recent advances in experimental measurements, CFD, and predictive models have strengthened thermal environment analysis in data centers. Yet most studies still examine these methods separately, and data exchange, cross-validation, and integrated use remain limited. Research is gradually shifting from isolated temperature or airflow assessment toward multiscale, multimethod integration and energy-efficiency optimization. Table 7 compares the three approaches in terms of typical outputs, strengths, reliability, limitations, and applications. The comparison is based on their commonly reported characteristics in previous studies, including data acquisition for experimental measurements [5,19], spatial representation for CFD simulations [47,66], and prediction efficiency and data requirements for predictive models [10,34]. These approaches are complementary rather than interchangeable, with distinct advantages in representing actual operation, resolving spatial fields, and reducing computation time.

Table 7. Comparison of experimental measurements, CFD, and predictive models.

Comparison Dimension	Experimental Measurement	CFD Numerical Simulation	Model Prediction
Typical outputs	Temperature and air velocity at cabinet inlets/outlets, hot/cold aisles, etc.	Full-field temperature distribution, Hotspot location and extent, Airflow organization and mixing	Key point temperature prediction Thermal risk assessment Temperature trend prediction
Main Advantages	Data is authentic and reliable, provides calibration data for simulation, mature technology	Obtains full spatial temperature distribution, can simulate extreme conditions, relatively low cost	Fast computation Low resource requirements Strong predictive capability
Main Limitations	Limited spatial coverage Measurement may cause interference, high cost	Oversimplifies real-world complexity High computational resource demands Relies on validation	Data-dependent accuracy, Poor scenario adaptability, Requires extensive training data, Weak physical interpretability
Reliability	High local fidelity	High field accuracy after validation	High in-domain approximation
Main uses	Monitoring, calibration, energy evaluation	Hotspot detection, airflow diagnosis, scheme comparison	Rapid assessment, parameter screening, online warning

Experimental measurements provide direct evidence of actual operating conditions. Measurements of temperature, air velocity, pressure, power, and energy use support operational monitoring, CFD boundary condition specification, model calibration, and energy performance assessment [5,32] When instruments are calibrated and measurement uncertainty is controlled, measurements offer high local fidelity. Their coverage is nevertheless constrained by sensor number and placement, test cost, and operating conditions, making full characterization of the three-dimensional thermal environment difficult [19]. Measurement design should therefore align parameter selection and sensor placement with the research objective and jointly capture the thermal environment, airflow organization, and cooling energy use.

CFD simulations provide continuous temperature, velocity, and pressure fields for hotspot identification, airflow organization diagnosis, and cooling-scheme comparison. Compared with discrete point measurements, they extend spatial and operating condition coverage and enable analysis under extreme boundary conditions. Their reliability is affected by boundary conditions, mesh settings, turbulence models, rack representation, and validation quality. Credible spatial field results require validation using variables and spatial scales consistent with the research objective [47]. Standardized model validation

and coupling with cooling-system models are therefore needed to extend CFD from thermal environment analysis to energy optimization.

Predictive models learn input–output relationships from measured or CFD data and rapidly estimate temperatures, hotspot risks, and thermal environment indicators for multi-condition assessment, parameter screening, and online early warning [16]. When trained on power or energy-use outputs, they can also predict energy performance. Compared with conventional CFD, predictive models are much faster, but their reliability is constrained by training data quality, sample coverage, and model structure. They generally provide accurate approximations within the training domain, but reliability may decline markedly beyond it. Further progress depends not only on algorithm complexity but also on hybrid frameworks that integrate physical laws, CFD data, and operational data.

The three methods therefore serve complementary roles: measurements provide the operational benchmark, CFD extends spatial and operating condition coverage, and predictive models enable rapid multi-condition analysis. For energy-efficiency assessment, measured power or energy-use data remain the most direct evidence. CFD mainly provides thermal environment and airflow constraints, whereas predictive models can estimate power or energy-use indicators only when trained on corresponding outputs.

6.2. Collaborative Framework for Experimental Measurement, CFD, and Predictive Modeling

Figure 13 shows the data flow, mutual validation, and iterative feedback among experimental measurements, CFD simulations, and predictive models. Measurements of temperature, air velocity, pressure, power, and energy use collected at rack inlets and outlets, in cold and hot aisles, and near cooling units provide the empirical basis for thermal environment assessment, CFD boundary condition definition, and model validation [32]. Measured power or energy-use data also directly support the evaluation of PUE and other energy performance indicators [44].

Once calibrated and validated against measurements, CFD models can generate multi-condition datasets covering different loads, supply-air temperatures, and airflow organization strategies, thereby extending the limited spatial and operating condition coverage of experiments [32]. The resulting temperature, velocity, and pressure fields support hotspot identification, airflow organization diagnosis, and cooling-scheme comparison, and they can also serve as training data for predictive models.

Predictive models can be trained on measurements and data generated by validated CFD models to rapidly estimate temperature fields, hotspot risks, and, where corresponding outputs are available, energy performance indicators. Their predictions can identify hotspots and steep temperature-gradient regions and, when uncertainty estimates are available, poorly represented operating conditions. These results can guide supplementary measurements and refine sensor placement. Substantial discrepancies between predictions and measurements should trigger a review of both the predictive and CFD models. Where CFD assumptions are responsible, boundary conditions, rack representations, or model parameters should be updated, and the revised CFD data, together with new measurements, can be used for model retraining.

Together, the three methods form an iterative framework based on data sharing, mutual validation, and discrepancy-driven updating. Experimental measurements provide the empirical benchmark, CFD expands spatial and operating condition coverage, and predictive models enable rapid assessment across multiple conditions. Their combined use can support thermal environment optimization and cooling-scheme screening, but energy-saving claims still require confirmation using measured power or energy-use data or a validated system-level energy model.

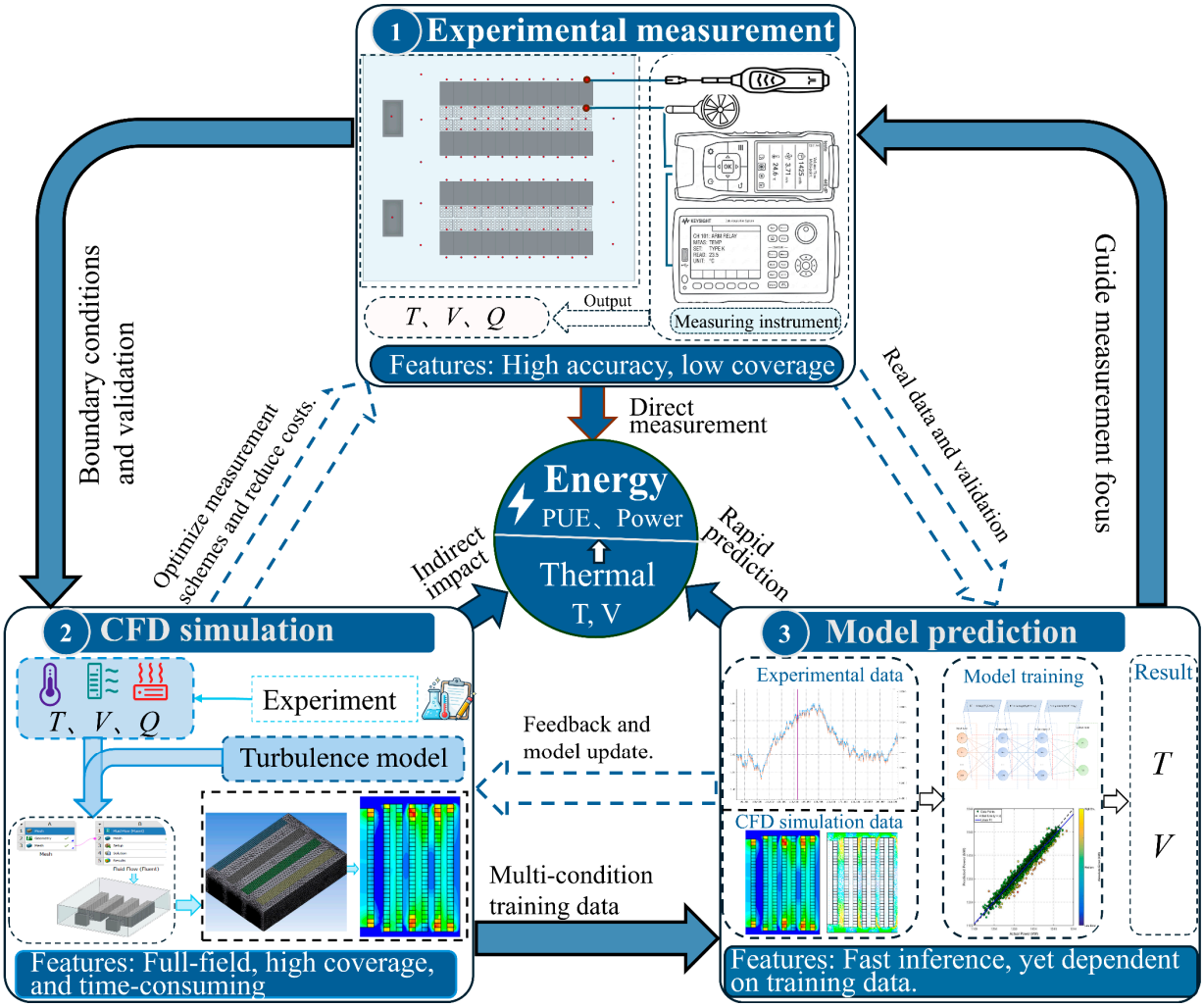


Figure 13. Schematic diagram of the synergistic relationship among experimental measurements, CFD simulations, and prediction models [71].

6.3. Challenges and Future Directions

Experimental measurements must capture representative multiscale behavior without significantly disrupting normal operation. Tradat et al. [19] showed that airflow estimates can vary with the method used for server- and rack-level measurements. Within racks, server fans, component layouts, and local flow paths create complex thermal and airflow patterns that sparse measurements cannot fully resolve. Large data centers also face high testing costs, limited access to operational data, and difficulty synchronizing multiple variables. Measurement campaigns should therefore coordinate sensor placement, parameter selection, and monitoring duration with the assessment objective rather than simply adding more sensors.

For CFD, the central trade-off is between model fidelity and computational cost. Results are affected by mesh resolution, turbulence models, server heat loads, rack airflow rates, and other boundary conditions. Liu et al. [57] emphasized the need for experimental calibration and validation, while larger computational domains and finer rack-level resolution rapidly increase cell count and runtime. Hu et al. [78] further reported that high-fidelity CFD cannot readily meet rapid-prediction requirements. Representing racks as uniform heat sources or black-box models may omit local thermal variations caused by server fans, internal airflow paths, and nonuniform heat sources [10]. Model scale should therefore match the research objective, with local mesh refinement and hierarchical modeling used to control computational cost.

Predictive models remain strongly dependent on their training domain. Fang et al. [10] showed that excessive simplification of racks and servers can discard important information on internal heat transfer and airflow, while Jin et al. [27] reported larger errors under off-design conditions. Most studies predict room-scale or rack-inlet temperatures; few resolve server-level hotspots or transient thermal responses within racks. Wang et al. [88] combined multiscale modeling with deep learning, but the resulting framework still requires validation under abrupt load changes, equipment failures, layout changes, and different cooling boundary conditions. Robust application therefore requires validation across loads, layouts, and boundary conditions, together with physical constraints during model training.

Beyond improving thermal prediction accuracy, future studies should further strengthen the connection between thermal performance assessment and energy performance evaluation. Current thermal studies mainly rely on temperature distribution, airflow characteristics, and hotspot indicators, whereas the impact of these improvements on cooling energy performance is less frequently quantified. Thermal optimization strategies may influence energy consumption through changes in airflow regulation, fan power, supply-air temperature, and cooling-system operation. Therefore, future frameworks should integrate thermal measurements, CFD simulations, and predictive models with energy-related parameters, including IT power, cooling-system power, airflow rate, and system-level efficiency indicators. Such thermal–energy coupling is essential for determining whether improved thermal conditions can translate into measurable energy benefits.

A further challenge is error propagation across the integrated workflow. When predictive models are trained on CFD data, uncertainties introduced by boundary condition specification, mesh discretization, and rack simplification may carry through to the final predictions. Differences in input variables, prediction targets, data partitioning, and evaluation metrics also limit direct comparison across studies [16]. Progress will require reusable multi-condition datasets, standardized validation protocols, cross-condition evaluation metrics, and explicit reporting of source-specific uncertainty and its propagation.

Improving any one method in isolation is therefore insufficient. A robust research framework requires objective-oriented measurements, validated multiscale CFD, and physics-informed predictive models, linked through uncertainty tracking and iterative recalibration.

7. Conclusions

This review analyzes 77 studies on data center thermal environments published since 2010, covering experimental measurements, CFD simulations, and predictive models. The key conclusions are as follows:

(1) Experimental measurements underpin thermal environment analysis and model validation, but current practices remain inconsistent. Temperature and air velocity were measured in 100% and 66.7% of the studies, respectively, whereas power, airflow rate, and pressure were less commonly monitored. A hierarchical measurement framework is therefore proposed for thermal safety assessment, airflow diagnosis, and model validation.

(2) Among 58 CFD studies, Fluent and 6SigmaDC were the dominant software platforms, while the standard k–ε model was the most widely used turbulence model. CFD expands spatial coverage relative to measurements, but its reliability depends on boundary conditions, model simplifications, and validation scope. Validation remains focused on temperature, with much less coverage of velocity and pressure, and thermal improvement alone does not demonstrate lower cooling energy use.

(3) The 17 prediction studies show that data-driven models can predict temperature fields and hotspot risks much faster than conventional CFD, but their performance remains limited by training data quality, operating condition coverage, and generalization. Future models should integrate measurements, data generated by validated CFD models, and physical constraints.

(4) The three methods are complementary: measurements provide real-world benchmarks, CFD expands spatial field and operating condition coverage, and predictive models enable rapid assessment. This review therefore proposes a closed-loop framework based on data sharing, mutual validation, and discrepancy-driven updating. Energy savings must still be confirmed using measured power or energy-use data or validated system-level models.

Author Contributions: methodology, H.T. and P.L.; software, H.T. and P.L.; validation, H.T. and P.L.; formal analysis, H.T., S.W., W.L. and P.L.; investigation, H.T.; writing—original draft preparation, H.T.; writing—review and editing, S.W., W.L. and P.L.; funding acquisition, P.L. All authors have read and agreed to the published version of the manuscript.

Funding: This work was supported by the National Natural Science Foundation of China (Grant No. 52568020) and the Science and Technology Planning Project of Qinghai Province (2025-ZJ-920Q).

Data Availability Statement: No new experimental data wedere generated in this study. The data analyzed in this review were obtained from the published literature cited in the article.

Conflicts of Interest: The authors declare no conflicts of interest.

Abbreviations

CFD	Computational Fluid Dynamics
IT	Information Technology
RCI	Rack Cooling Index
SHI	Supply Heat Index
RHI	Return Heat Index
RTI	Return Temperature Index
PUE	Power Usage Effectiveness
ML	Machine Learning
GPR	Gaussian Process Regression
ANN	Artificial Neural Network
POD	Proper Orthogonal Decomposition
FNM	Flow Network Method
MDF	Model-Driven Framework
DDF	Data-Driven Framework
A-PCNN	Adaptive Physically Consistent Neural Networks
ADB	Attention–DNN–Bayesian model
DNN	Deep Neural Network
GA	Genetic Algorithm
MAPE	Mean Absolute Percentage Error
MSE	Mean Squared Error

References

1. Alkharabsheh, S.; Fernandes, J.; Gebrehiwot, B.; Agonafer, D.; Ghose, K.; Ortega, A.; Joshi, Y.; Sammakia, B. A brief overview of recent developments in thermal management in data centers. *J. Electron. Packag.* **2015**, *137*, 040801. https://doi.org/10.1115/1.4031326.
2. Meng, X.; Zhou, J.; Zhang, X.; Luo, Z.; Gong, H.; Gan, T. Optimization of the thermal environment of a small-scale data center in China. *Energy* **2020**, *196*, 117080. https://doi.org/10.1016/j.energy.2020.117080.

3. Kumar, P.; Sundaralingam, V.; Joshi, Y.; Patterson, M.K.; Steinbrecher, R.; Mena, M. Effect of supply air temperature on rack cooling in a high density raised floor data center facility. In Proceedings of the ASME 2011 International Mechanical Engineering Congress and Exposition, Denver, CO, USA, 11–17 November 2011; pp. 1369–1380. https://doi.org/10.1115/IMECE2011-65574.
4. Nada, S.A.; Said, M.A. Effect of CRAC units layout on thermal management of data center. *Appl. Therm. Eng.* **2017**, *118*, 339–344. https://doi.org/10.1016/j.applthermaleng.2017.03.003.
5. Fulpagare, Y.; Hsu, P.-H.; Wang, C.-C. Experimental analysis of airflow uniformity and energy consumption in data centers. *Appl. Therm. Eng.* **2022**, *209*, 118302. https://doi.org/10.1016/j.applthermaleng.2022.118302.
6. Cruz, E.; Joshi, Y.; Iyengar, M.; Schmidt, R. Comparison of numerical modeling to experimental data in a small data center test cell. In Proceedings of the ASME 2009 International Electronic Packaging Technical Conference and Exhibition, San Francisco, CA, USA, 19–23 July 2009; pp. 953–961. https://doi.org/10.1115/InterPACK2009-89306.
7. Yuan, X.; Zhou, X.; Liu, J.; Wang, Y.; Kosonen, R.; Xu, X. Experimental and numerical investigation of an airflow management system in data center with lower-side terminal baffles for servers. *Build. Environ.* **2019**, *155*, 308–319. https://doi.org/10.1016/j.buildenv.2019.03.039.
8. Cho, J.; Park, C.; Choi, W. Numerical and experimental study of air containment systems in legacy data centers focusing on thermal performance and air leakage. *Case Stud. Therm. Eng.* **2021**, *26*, 101084. https://doi.org/10.1016/j.csite.2021.101084.
9. Athavale, J.; Joshi, Y.; Yoda, M. Artificial neural network based prediction of temperature and flow profile in data centers. In Proceedings of the 17th IEEE Intersociety Conference on Thermal and Thermomechanical Phenomena in Electronic Systems (ITherm), San Diego, CA, USA, 29 May–1 June 2018; pp. 871–880.
10. Fang, L.; Xu, Q.; Li, S.; Xia, Y.; Chen, Q. Temperature prediction in data center combining with deep neural network. *Appl. Therm. Eng.* **2024**, *244*, 122571. https://doi.org/10.1016/j.applthermaleng.2024.122571.
11. Liu, Y.; Zhou, C.; Hu, Y.; Zhang, W.; He, W.; Guan, W. An ANN–CNN Hybrid Surrogate Model for Fast Prediction of 3D Temperature Fields in Large Datacenter Rooms. *Buildings* **2025**, *15*, 4042. https://doi.org/10.3390/buildings15224042.
12. Song, P.; Zhang, Z.; Zhu, Y. Numerical and experimental investigation of thermal performance in data center with different deflectors for cold aisle containment. *Build. Environ.* **2021**, *200*, 107961. https://doi.org/10.1016/j.buildenv.2021.107961.
13. Zhang, Z.; Niu, B.; Zhang, Z.; Shi, M. Optimization on jet-induced ventilation to enhance the uniformity of airflow distribution in data center. *Energy Sci. Eng.* **2021**, *9*, 1973–1996. https://doi.org/10.1002/ese3.986.
14. Gao, C.; Yu, Z.; Wu, J. Investigation of airflow pattern of a typical data center by CFD simulation. In Proceedings of the 6th International Building Physics Conference (IBPC 2015), Torino, Italy, 14–17 June 2015; pp. 2687–2693. https://doi.org/10.1016/j.egypro.2015.11.350.
15. Yu, F.; Chen, H.; Wang, W.; An, J. Optimization Strategies for Underfloor Air Distribution in a Small-Scale Data Center. *Buildings* **2025**, *15*, 428. https://doi.org/10.3390/buildings15030428.
16. Athavale, J.; Yoda, M.; Joshi, Y. Comparison of data driven modeling approaches for temperature prediction in data centers. *Int. J. Heat Mass Transf.* **2019**, *135*, 1039–1052. https://doi.org/10.1016/j.ijheatmasstransfer.2019.02.041.
17. Cho, J.; Woo, J.; Park, B.; Lim, T. A comparative CFD study of two air distribution systems with hot aisle containment in high-density data centers. *Energies* **2020**, *13*, 6147. https://doi.org/10.3390/en13226147.
18. Szeliga, W.; Oleksiak, A.; Roszak, R.; Górzeński, R. CFD4DC: Automated CFD framework for heat transfer analysis of data centers. *Appl. Therm. Eng.* **2026**, *283*, 128982. https://doi.org/10.1016/j.applthermaleng.2025.128982.
19. Tradat, M.; Mohsenian, G.; Manaserh, Y.; Sammakia, B.; Mendo, D.; Alissa, H.A. Experimental Analysis of Different Measurement Techniques of Server-Rack Airflow Predictions Towards Proper DC Airflow Management. In Proceedings of the 2020 19th IEEE Intersociety Conference on Thermal and Thermomechanical Phenomena in Electronic Systems (ITherm), Online, 21–23 July 2020; pp. 366–373. https://doi.org/10.1109/itherm45881.2020.9190584.
20. Kuzay, M.; Dogan, A.; Yilmaz, S.; Herkiloglu, O.; Atalay, A.S.; Cemberci, A.; Yilmaz, C.; Demirel, E. Numerical and experimental dataset for a retrofitted data center. *Data Brief* **2022**, *45*, 108587. https://doi.org/10.1016/j.dib.2022.108587.
21. Wu, L.; Mao, R.; Wu, H.; Zhang, J.; Li, C.; Yi, X.; Huang, G.; Zhang, Z. Optimization of airflow organization in fan-wall data center via baffles. *Appl. Therm. Eng.* **2024**, *244*, 122745. https://doi.org/10.1016/j.applthermaleng.2024.122745.
22. Singh, N.; Permana, I.; Helal, H.H.S.; Wei, C.-C.; Wang, F.-J. Performance improvement approach for retrofitting a data center. *J. Build. Eng.* **2025**, *111*, 113238. https://doi.org/10.1016/j.jobe.2025.113238.
23. Cho, J.; Park, B.; Jeong, Y.; Lee, S. Thermal performance evaluation of a high-density data centre for cooling system under fault conditions. *Proc. E3S Web Conf.* **2019**, *111*, 01043. https://doi.org/10.1051/e3sconf/201911101043.
24. Cao, S.; Wu, T.; Ling, J.; Wu, L. Optimizing server inlet areas for enhanced thermal management in data centers: A CFD-based investigation. *Int. Commun. Heat Mass Transf.* **2025**, *168*, 109432. https://doi.org/10.1016/j.icheatmasstransfer.2025.109432.

25. Tarutani, Y.; Hashimoto, K.; Hasegawa, G.; Nakamura, Y.; Tamura, T.; Matsuda, K.; Matsuoka, M. Temperature distribution prediction in data centers for decreasing power consumption by machine learning. In Proceedings of the 2015 IEEE 7th International Conference on Cloud Computing Technology and Science (CloudCom), Vancouver, BC, Canada, 30 November–3 December 2015; pp. 635–642. https://doi.org/10.1109/CloudCom.2015.49.
26. Lin, J.; Lin, W.; Lin, W.; Wang, J.; Jiang, H. Thermal prediction for air-cooled data center using data driven-based model. *Appl. Therm. Eng.* **2022**, *217*, 119207. https://doi.org/10.1016/j.applthermaleng.2022.119207.
27. Jin, S.-Q.; Li, N.; Bai, F.; Chen, Y.-J.; Feng, X.-Y.; Li, H.-W.; Gong, X.-M.; Tao, W.-Q. Data-driven model reduction for fast temperature prediction in a multi-variable data center. *Int. Commun. Heat Mass Transf.* **2023**, *142*, 106645. https://doi.org/10.1016/j.icheatmasstransfer.2023.106645.
28. Tang, Y.-Q.; Fang, W.-Z.; Zheng, C.-Y.; Tao, W.-Q. Applications of POD-based reduced order model to the rapid prediction of velocity and temperature in data centers. *Appl. Therm. Eng.* **2025**, *263*, 125310. https://doi.org/10.1016/j.applthermaleng.2024.125310.
29. Deng, P.; Xu, Q.; Zhu, X.; Dong, W. CFD-based data-driven machine learning temperature prediction: Case study on a 180-rack server room within a large-scale data center. *Int. J. Therm. Sci.* **2026**, *221*, 110465. https://doi.org/10.1016/j.ijthermalsci.2025.110465.
30. Chen, D.; Chui, C.-K.; Lee, P.S. Adaptive physically consistent neural networks for data center thermal dynamics modeling. *Appl. Energy* **2025**, *377*, 124637. https://doi.org/10.1016/j.apenergy.2024.124637.
31. Song, Z. Numerical cooling performance evaluation of fan-assisted perforations in a raised-floor data center. *Int. J. Heat Mass Transf.* **2016**, *95*, 833–842. https://doi.org/10.1016/j.ijheatmasstransfer.2015.12.060.
32. Wang, F.; Huang, Y.; Prasetyo, B. Energy-efficient improvement approaches through numerical simulation and field measurement for a data center. *Energies* **2019**, *12*, 2757. https://doi.org/10.3390/en12142757.
33. Han, X.; Tian, W.; VanGilder, J.; Zuo, W.; Faulkner, C. An open source fast fluid dynamics model for data center thermal management. *Energy Build.* **2021**, *230*, 110599. https://doi.org/10.1016/j.enbuild.2020.110599.
34. Dai, Y.; Zhao, J.; Zhang, X.; Bai, F.; Tao, W.; Wang, Y. Thermal full-field prediction of an air-cooled data center using a novel multi-scale approach based on POD and CFD coupling. *Energy Build.* **2024**, *307*, 113992. https://doi.org/10.1016/j.enbuild.2024.113992.
35. Guo, H.-B.; Chen, J.-Y.; Li, Z.-D.; Liu, X.-H.; Li, N.; Tao, W.-Q. FNM-based rack model and CFD-FNM coupling framework for data center rack-level simulation. *Build. Environ.* **2025**, *272*, 112675. https://doi.org/10.1016/j.buildenv.2025.112675.
36. Lu, H.; Zhang, Z.; Yang, L. A review on airflow distribution and management in data center. *Energy Build.* **2018**, *179*, 264–277. https://doi.org/10.1016/j.enbuild.2018.08.050.
37. Chu, W.; Wang, C. A review on airflow management in data centers. *Appl. Energy* **2019**, *240*, 84–119. https://doi.org/10.1016/j.apenergy.2019.02.041.
38. Jin, C.; Bai, X.; Yang, C. Effects of airflow on the thermal environment and energy efficiency in raised-floor data centers: A review. *Sci. Total Environ.* **2019**, *695*, 133801. https://doi.org/10.1016/j.scitotenv.2019.133801.
39. Zhao, R.; Du, Y.; Yang, X.; Zhou, Z.; Wang, W.; Yang, X. A critical review on the thermal management of data center for local hotspot elimination. *Energy Build.* **2023**, *297*, 113486. https://doi.org/10.1016/j.enbuild.2023.113486.
40. Zhang, Q.; Meng, Z.; Hong, X.; Zhan, Y.; Liu, J.; Dong, J.; Bai, T.; Niu, J.; Deen, A. A survey on data center cooling systems: Technology, power consumption modeling and control strategy optimization. *J. Syst. Archit.* **2021**, *119*, 102253. https://doi.org/10.1016/j.sysarc.2021.102253.
41. Ahmed, K.; Bollen, M.; Alvarez, M. A Review of Data Centers Energy Consumption and Reliability Modeling. *IEEE Access* **2021**, *9*, 152536–152563. https://doi.org/10.1109/access.2021.3125092.
42. Herrlin, M.K. Rack cooling effectiveness in data centers and telecom central offices: The rack cooling index (RCI). *ASHRAE Trans.* **2005**, *111*, 725–731.
43. Cho, J.; Yang, J.; Park, W. Evaluation of air distribution system's airflow performance for cooling energy savings in high-density data centers. *Energy Build.* **2014**, *68*, 270–279. https://doi.org/10.1016/j.enbuild.2013.09.013.
44. Choo, K.; Galante, R.M.; Ohadi, M.; Cooper, D. Measured and simulated energy consumption analysis of a data center on an academic campus. In Proceedings of the 29th Annual IEEE Semiconductor Thermal Measurement and Management Symposium (SEMI-THERM), San Jose, CA, USA, 17–21 March 2013; pp. 231–236. https://doi.org/10.1109/SEMI-THERM.2013.6526834.
45. Nada, S.A.; Said, M.A.; Rady, M.A. Numerical investigation and parametric study for thermal and energy management enhancements in data centers' buildings. *Appl. Therm. Eng.* **2016**, *98*, 110–128. https://doi.org/10.1016/j.applthermaleng.2015.12.020.

46. Alissa, H.A.; Nemati, K.; Sammakia, B.; Ghose, K.; Seymour, M.; Schmidt, R. Innovative approaches of experimentally guided CFD modeling for data centers. In Proceedings of the 31st Annual Semiconductor Thermal Measurement, Modeling and Management Symposium (SEMI-THERM), San Jose, CA, USA, 15–19 March 2015; pp. 176–184. https://doi.org/10.1109/SEMI-THERM.2015.7100157.
47. Wibron, E.; Ljung, A.-L.; Lundström, T.S. Computational fluid dynamics modeling and validating experiments of airflow in a data center. *Energies* **2018**, *11*, 644. https://doi.org/10.3390/en11030644.
48. Yuan, X.; Wang, Y.; Liu, J.; Xu, X.; Yuan, X. Experimental and numerical study of airflow distribution optimisation in high-density data centre with flexible baffles. *Build. Environ.* **2018**, *140*, 128–139. https://doi.org/10.1016/j.buildenv.2018.05.043.
49. Dogan, A.; Yilmaz, S.; Kuzay, M.; Demirel, E. Development and validation of an open-source CFD model for the efficiency assessment of data centers. *Open Res. Eur.* **2022**, *2*, 41. https://doi.org/10.12688/openreseurope.14579.1.
50. Kuzay, M.; Dogan, A.; Yilmaz, S.; Herkiloglu, O.; Atalay, A.S.; Cemberci, A.; Yilmaz, C.; Demirel, E. Retrofitting of an air-cooled data center for energy efficiency. *Case Stud. Therm. Eng.* **2022**, *36*, 102228. https://doi.org/10.1016/j.csite.2022.102228.
51. Nada, S.A.; Said, M.A.; Rady, M.A. CFD investigations of data centers' thermal performance for different configurations of CRAC units and aisle separation. *Alex. Eng. J.* **2016**, *55*, 959–971. https://doi.org/10.1016/j.aej.2016.02.025.
52. Chu, W.-X.; Wang, C.-C. CFD investigation of airflow management in a small container data center. *IEEE Trans. Compon. Packag. Manuf. Technol.* **2019**, *9*, 2177–2188. https://doi.org/10.1109/tcpmt.2019.2916017.
53. Lu, H.; Zhang, Z. Numerical and experimental investigations on the thermal performance of a data center. *Appl. Therm. Eng.* **2020**, *180*, 115759. https://doi.org/10.1016/j.applthermaleng.2020.115759.
54. Tradat, M.I.; Manaserh, Y.M.A.; Sammakia, B.G.; Hoang, C.H.; Alissa, H.A. An experimental and numerical investigation of novel solution for energy management enhancement in data centers using underfloor plenum porous obstructions. *Appl. Energy* **2021**, *289*, 116663. https://doi.org/10.1016/j.apenergy.2021.116663.
55. Tang, Y.; Bai, X.; Jin, C.; Fu, Y.; Mao, W.; Xu, X. Experimental and numerical study on the thermal environment of a data center. *Build. Environ.* **2022**, *212*, 108741. https://doi.org/10.1016/j.buildenv.2021.108741.
56. Saiyad, A.; Fulpagare, Y.; Bhargav, A. Comparison of detached eddy simulation and standard k−ε RANS model for rack-level airflow analysis inside a data center. *Build. Simul.* **2022**, *15*, 1595–1610. https://doi.org/10.1007/s12273-021-0879-3.
57. Liu, W.; Lian, S.; Fang, X.; Shang, Z.; Wu, H.; Zhu, H.; Hu, S. An open-source and experimentally guided CFD strategy for predicting air distribution in data centers with air-cooling. *Build. Environ.* **2023**, *242*, 110542. https://doi.org/10.1016/j.buildenv.2023.110542.
58. Fulpagare, Y.; Joshi, Y.; Bhargav, A. Rack level transient CFD modeling of data center. *Int. J. Numer. Methods Heat Fluid Flow* **2018**, *28*, 381–394. https://doi.org/10.1108/HFF-10-2016-0426.
59. Khalaj, A.H.; Scherer, T.; Siriwardana, J.; Halgamuge, S. Increasing the thermal efficiency of an operational data center using cold aisle containment. In Proceedings of the IEEE 7th International Conference on Information and Automation for Sustainability (ICIAfS), Colombo, Sri Lanka, 22–24 December 2014. https://doi.org/10.1109/ICIAFS.2014.7069633.
60. Pardey, Z.M.; VanGilder, J.W.; Healey, C.M.; Plamondon, D.W. Creating a calibrated CFD model of a midsize data center. In Proceedings of the ASME 2015 International Technical Conference and Exhibition on Packaging and Integration of Electronic and Photonic Microsystems and ASME 2015 13th International Conference on Nanochannels, Microchannels, and Minichannels (InterPACK/ICNMM 2015), San Francisco, CA, USA, 6–9 July 2015; p. V001T09A029. https://doi.org/10.1115/IPACK2015-48448.
61. Pico, P.; Valdés, J.P.; Pinilla, A.; Echeverri, A.; Gómez, J.M.; Ratkovich, N.; Cifuentes, B. CFD modelling of the air conditioning system for a Tier 2 Data Centre. *Adv. Build. Energy Res.* **2022**, *16*, 231–261. https://doi.org/10.1080/17512549.2020.1860818.
62. Abdelmaksoud, W.A.; Khalifa, H.E.; Dang, T.Q.; Schmidt, R.R.; Iyengar, M. Improved CFD modeling of a small data center test cell. In Proceedings of the 2010 12th IEEE Intersociety Conference on Thermal and Thermomechanical Phenomena in Electronic Systems (ITHERM), Las Vegas, NV, USA, 2–5 June 2010; pp. 1–9. https://doi.org/10.1109/ITHERM.2010.5501425.
63. Le, D.; Liu, Y.; Wang, R.; Tan, R.; Wong, Y.; Wen, Y. Control of air free-cooled data centers in tropics via deep reinforcement learning. In Proceedings of the 6th ACM International Conference on Systems for Energy-Efficient Built Environments (BuildSys), New York, NY, USA, 13–14 November 2019; pp. 306–315. https://doi.org/10.1145/3360322.3360845.
64. Fulpagare, Y.; Bhargav, A.; Joshi, Y. Dynamic thermal characterization of raised floor plenum data centers: Experiments and CFD. *J. Build. Eng.* **2019**, *25*, 100783. https://doi.org/10.1016/j.jobe.2019.100783.
65. Wu, L.; Mao, R.; Zhang, J.; Li, C.; Gan, J.; Zhou, J.; Zhang, Z. An experimental study on improving the thermal environment of data centers by optimizing fan wall arrangement. *J. Build. Eng.* **2024**, *96*, 110421. https://doi.org/10.1016/j.jobe.2024.110421.

66. Sarikaya, O.M.; Kuzay, M.; Demirel, E.; Melgaard, S.P.; Nielsen, J.E.; Jensen, R.L.; Oleksiak, A.; Szeliga, W. Energy efficiency enhancement in two European data centers through CFD modeling. *Sci. Rep.* **2025**, *15*, 24952. https://doi.org/10.1038/s41598-025-11048-0.
67. Hassan, N.M.S.; Khan, M.M.K.; Rasul, M.G. Temperature monitoring and CFD analysis of data centre. *Procedia Eng.* **2013**, *56*, 551–559. https://doi.org/10.1016/j.proeng.2013.03.159.
68. Ni, J.; Jin, B.; Zhang, B.; Wang, X. Simulation of thermal distribution and airflow for efficient energy consumption in a small data centers. *Sustainability* **2017**, *9*, 664. https://doi.org/10.3390/su9040664.
69. Sheth, D.V.; Saha, S.K. Numerical study of thermal management of data centre using porous medium approach. *J. Build. Eng.* **2019**, *22*, 200–215. https://doi.org/10.1016/j.jobe.2018.12.012.
70. Guo, Y.; Zhao, C.; Gao, H.; Shen, C.; Fu, X. Improving thermal performance in data centers based on numerical simulations. *Buildings* **2024**, *14*, 1416. https://doi.org/10.3390/buildings14051416.
71. Macedo, D.; Godina, R.; Gaspar, P.D.; Silva, P.; Covas, M.T. A parametric numerical study of the airflow and thermal performance in a real data center for improving sustainability. *Appl. Sci.* **2019**, *9*, 3850. https://doi.org/10.3390/app9183850.
72. Zhang, B.; Liao, W.; Li, X.; Li, Z. Rapid prediction of air temperature distribution in data center via feature-integrated machine learning. *Energy Build.* **2025**, *342*, 115891. https://doi.org/10.1016/j.enbuild.2025.115891.
73. Durand-Estebe, B.; Le Bot, C.; Mancos, J.N.; Arquis, E. Data center optimization using PID regulation in CFD simulations. *Energy Build.* **2013**, *66*, 154–164. https://doi.org/10.1016/j.enbuild.2013.07.053.
74. Fulpagare, Y.; Mahamuni, G.; Bhargav, A. Effect of plenum chamber obstructions on data center performance. *Appl. Therm. Eng.* **2015**, *80*, 187–195. https://doi.org/10.1016/j.applthermaleng.2015.01.065.
75. Zhou, C.; Yang, C.; Wang, C.; Zhang, X. Numerical simulation on a thermal management system for a small data center. *Int. J. Heat Mass Transf.* **2018**, *124*, 677–692. https://doi.org/10.1016/j.ijheatmasstransfer.2018.04.005.
76. Yang, T.-F.; Chen, Y.-C.; Chen, B.-L.; Li, C.-H.; Yan, W.-M. Numerical study of fluid flow and temperature distributions in a data center. *Case Stud. Therm. Eng.* **2021**, *28*, 101405. https://doi.org/10.1016/j.csite.2021.101405.
77. Barestrand, H.; Ljung, A.-L.; Summers, J.; Lundström, S. Modeling convective heat transfer of air in a data center using OpenFOAM: Evaluation of the Boussinesq buoyancy approximation. *OpenFOAM® J.* **2023**, *3*, 146–158. https://doi.org/10.51560/ofj.v3.59.
78. Hu, B.; Yin, Z.; Hamrani, A.; Leon, A.; McDaniel, D. Super-resolution-assisted rapid high-fidelity CFD modeling of data centers. *Build. Environ.* **2024**, *247*, 111036. https://doi.org/10.1016/j.buildenv.2023.111036.
79. Bong, R.E.J.; Sivasankaran, P.N.; Muniandy, N.; Jayatilleke, B.; Kanesavathanan. To simulate the air flow and temperature distribution for a data centre. *J. Phys. Conf. Ser.* **2024**, *2923*, 012016. https://doi.org/10.1088/1742-6596/2923/1/012016.
80. Bai, F.; Gong, X.-M.; Li, H.-W.; Guo, H.-B.; Tao, W.-Q. An improved black box model and the details of its numerical treatments for rack in data center simulation. *Int. Commun. Heat Mass Transf.* **2024**, *158*, 107916. https://doi.org/10.1016/j.icheatmasstransfer.2024.107916.
81. Arghode, V.K.; Joshi, Y. Modeling strategies for air flow through perforated tiles in a data center. *IEEE Trans. Compon. Packag. Manuf. Technol.* **2013**, *3*, 800–810. https://doi.org/10.1109/tcpmt.2013.2251058.
82. Watson, B.; Venkiteswaran, V.K. Universal cooling of data centres: A CFD analysis. *Energy Procedia* **2017**, *142*, 2711–2720. https://doi.org/10.1016/j.egypro.2017.12.215.
83. Wulandari, D.A.; Akmal, M.; Gunawan, Y.; Nasruddin. Cooling improvement of the IT rack by layout rearrangement of the A2 class data center room: A simulation study. *Evergreen* **2020**, *7*, 489–499. https://doi.org/10.5109/4150468.
84. Lee, M.D.; Michael, Z.; Makarem, M.A.; Samsudin, A.H. Computational fluid dynamics analysis of cooling strategies for data center thermal optimization. *Int. Commun. Comput. Mech.* **2025**, *3*, 28–38.
85. Gong, X.; Chen, J.; Liu, X.; Ying, H.; Xue, X.; Dai, Y.; Tao, W. Study on three numerical models for rack in data center and comparisons with test results. *Energy Build.* **2026**, *359*, 117302. https://doi.org/10.1016/j.enbuild.2026.117302.
86. Chen, H.; Li, D.; Wang, S.; Chen, T.; Zhong, M.; Ding, Y.; Li, Y.; Huo, X. Numerical investigation of thermal performance with adaptive terminal devices for cold aisle containment in data centers. *Buildings* **2023**, *13*, 268. https://doi.org/10.3390/buildings13020268.
87. Asgari, S.; Moazamigoodarzi, H.; Tsai, P.J.; Pal, S.; Zheng, R.; Badawy, G.; Puri, I.K. Hybrid surrogate model for online temperature and pressure predictions in data centers. *Future Gener. Comput. Syst.* **2021**, *114*, 531–547. https://doi.org/10.1016/j.future.2020.08.029.

88. Wang, N.; Guo, Y.; Huang, C.; Tian, B.; Shao, S. Multi-scale collaborative modeling and deep learning-based thermal prediction for air-cooled data centers: An innovative insight for thermal management. *Appl. Energy* **2025**, *377*, 124568. https://doi.org/10.1016/j.apenergy.2024.124568.
89. Wang, Y.; Zhang, Y.; Nörtershäuser, D.; Le Masson, S.; Menaud, J. Model and data driven transient thermal system modelings for contained data centers. *Energy Build.* **2022**, *258*, 111790. https://doi.org/10.1016/j.enbuild.2021.111790.
90. Kuwahara, H.; Hsu, Y.-F.; Matsuda, K.; Matsuoka, M. Dynamic power consumption prediction and optimization of data center by using deep learning and computational fluid dynamics. In Proceedings of the IEEE 7th International Conference on Cloud Networking (CloudNet), Tokyo, Japan, 22–24 October 2018. https://doi.org/10.1109/CloudNet.2018.8549256.
91. Saiyad, A.; Patel, A.; Fulpagare, Y.; Bhargav, A. Predictive modeling of thermal parameters inside the raised floor plenum data center using artificial neural networks. *J. Build. Eng.* **2021**, *42*, 102397. https://doi.org/10.1016/j.jobe.2021.102397.
92. Omrani, M.; Ghassemi, M. AI-driven optimization of fan-wall cooling system in a medium-density data center. *Int. J. Heat Mass Transf.* **2025**, *247*, 127159. https://doi.org/10.1016/j.ijheatmasstransfer.2025.127159.

Disclaimer/Publisher's Note: The statements, opinions and data contained in all publications are solely those of the individual author(s) and contributor(s) and not of MDPI and/or the editor(s). MDPI and/or the editor(s) disclaim responsibility for any injury to people or property resulting from any ideas, methods, instructions or products referred to in the content.